Several studies have recently implicated another functional significance of NIK protein in epithelial cell proliferation, inflammatory response, and oncogenic signaling (for review, see Thu and Richmond, 2010). Although the expression level of NIK is strictly maintained by proteasomal degradation in normal cells (Liao et al., 2004), increased level of NIK transcript are observed in some cancers, causing inappropriate accumulation of NIK protein without stimuli (Annunziata et al., 2007; Saitoh et al., 2008). Overexpression of NIK leads to aberrant phenotypes in several cell types; however, little is known about the abnormal accumulation of NIK in malignant cells.

Recent advances have led to deeper understanding of a new aspect of posttranscriptional gene regulation, i.e., regulation by a class of noncoding RNAs. MicroRNAs (miRNAs) are functional RNAs with 18–25 nt in length that contribute to a class of cellular functions by negatively controlling targeted gene expression via base-pairing to 3′ untranslated region (3′ UTR). A single miRNA regulates the expression of multiple genes, and the functions of miRNAs therefore need to be orchestrated for cellular homeostasis (Ventura and Jacks, 2009). In the context of cancer pathology, many studies have provided evidences that miRNAs can act as either oncogenes or tumor suppressors. Although the relationship between miRNA deregulation and oncogenes has been clarified in several cancer cells, there has been no integrated analysis of gene expression in ATL. Since miRNAs have important functions in living cells, miRNA expression needs to be tightly regulated. Our knowledge about the regulatory mechanisms of miRNA expression is very inadequate because research effort has focused mainly on the role of miRNAs, which remains one of the most intriguing questions. miRNA regulation involves multiple steps. miRNA maturation has been identified as an important step, and its deregulation leads to progression and development of cancer (Davis et al., 2008; Trabucchi et al., 2009). Genetic deletion in cancer cells has also been reported to account for specific miRNA defect (Varambally et al., 2008). In addition, miRNA expression seems to be epigenetically programmed. DNA methylation and histone modification are strong candidates for miRNA regulation and their abnormalities, therefore, have causal roles in cancer initiation, development, and progression. In particular, Polycomb group proteins have central functions in cellular development and regeneration by controlling histone methylation, especially at histone H3 Lys27 (H3K27), which induces chromatin compaction (Simon and Kingston, 2009). Recent studies have revealed that the amount of Polycomb family is closely associated with cancer phenotypes and malignancy in breast cancer, prostate cancer, and other neoplasms (Sparmann and van Lohuizen, 2006). However, the substantial status of Polycomb family and their epigenetic impact in ATL cells have not been documented. Furthermore, the general roles of Polycomb proteins in miRNA regulation are mostly unknown. As described above, since miRNAs are multifunctional molecules in gene regulation, it is of pivotal importance to clarify the miRNAs functions and their regulatory circuit in order to formulate therapeutic strategies.

In the present study, we first performed global miRNA and mRNA profilings of the ATL cells derived from patients to precisely define the significance of miRNA expressions and functions.

RESULTS

miRNA Expression Signature in Primary ATL Cells

To characterize the miRNA expression signature in the primary ATL cells, we first performed an miRNA expression microarray analysis. For results with physiological significance, we used total RNA prepared from clinical ATL samples (n = 40, Table S1 available online) and control CD4+ T cells from healthy donors (n = 22) aged 50–70 years. A strict threshold ($p < 1 \times 10^{-5}$) and two-dimensional hierarchical clustering analysis revealed 61 miRNAs that showed significantly altered levels of expression in ATL cells compared with those of control CD4+ T cells (Figure 1A). It is noteworthy that 59 miRNAs out of 61 (96.7%) showed decreased expression in the primary ATL cells. Among them, we identified miR-31 as one of the most profoundly repressed miRNAs in all ATL individuals (fold change, 0.00403; Figure 1B). miR-31 was recently reported as a tumor suppressor and/or metastasis-associated miRNA in metastatic breast cancer. However, the biological functions of miR-31 in lymphocytes have not been studied. We therefore focused on the biological significance and regulatory mechanisms of miR-31 expression in T cells as well as in solid cancers.

miR-31 Negatively Regulates NF-κB Signaling via NIK Expression

To study the functional significance of miR-31 loss, we attempted to identify the target genes of miR-31 using four computational algorithms. We also performed gene expression microarray analysis of the primary ATL cells (n = 52, Table S1) and normal CD4+ T cells (n = 21) in order to detect aberrations in gene expression. Selected putative target genes are known to be involved in cell-cycle regulation and T cell development (Table S2). To experimentally identify the target genes, we performed reporter-based screens as described below. Luciferase-3′ UTR reporter assays demonstrated a remarkable negative effect against upstream gene expression by the *MAP3K14* 3′ UTR sequence (Figure S1B), which is consistent with an initial cloning report (Malinin et al., 1997). MAP3K14, also known as NIK, has a central role in noncanonical NF-κB signaling by phosphorylation of IKKα. A previous report (Saitoh et al., 2008) and the present results (Table S2) show that NIK is overexpressed in ATL cells, leading to constitutive NF-κB activation. As shown in Figure 2A, treatment with a miR-31 inhibitor increased *NIK* 3′ UTR reporter activity, suggesting the involvement of endogenous miR-31 in NIK downregulation. A computational search predicted one site each of miR-31 and miR-31 antisense (miR-31*) binding sites in the *NIK* 3′ UTR (Figure 2B). To identify the regulatory sequence in 3′ UTR of *NIK*, we established additional two reporters with mutated sequence in each potential seed region (Figure 2C; Figure S1C). Mutant 1, which contains mutated sequence in the miR-31 seed region, partially canceled the negative effect of endogenous miR-31 (Figure S1D) and prevented the effect of Anti-miR-31 treatment (Figure 2D). On the contrary, our results suggest that miR-31* does not participate in NIK regulation. miR-31-mediated reporter regulation was also observed in T cell lines (Figure S1E). To confirm the results, we repeated the experiment to examine whether miR-31 could inhibit NIK expression through seed sequence. We made expression plasmid vectors carrying NIK, NIK-3′

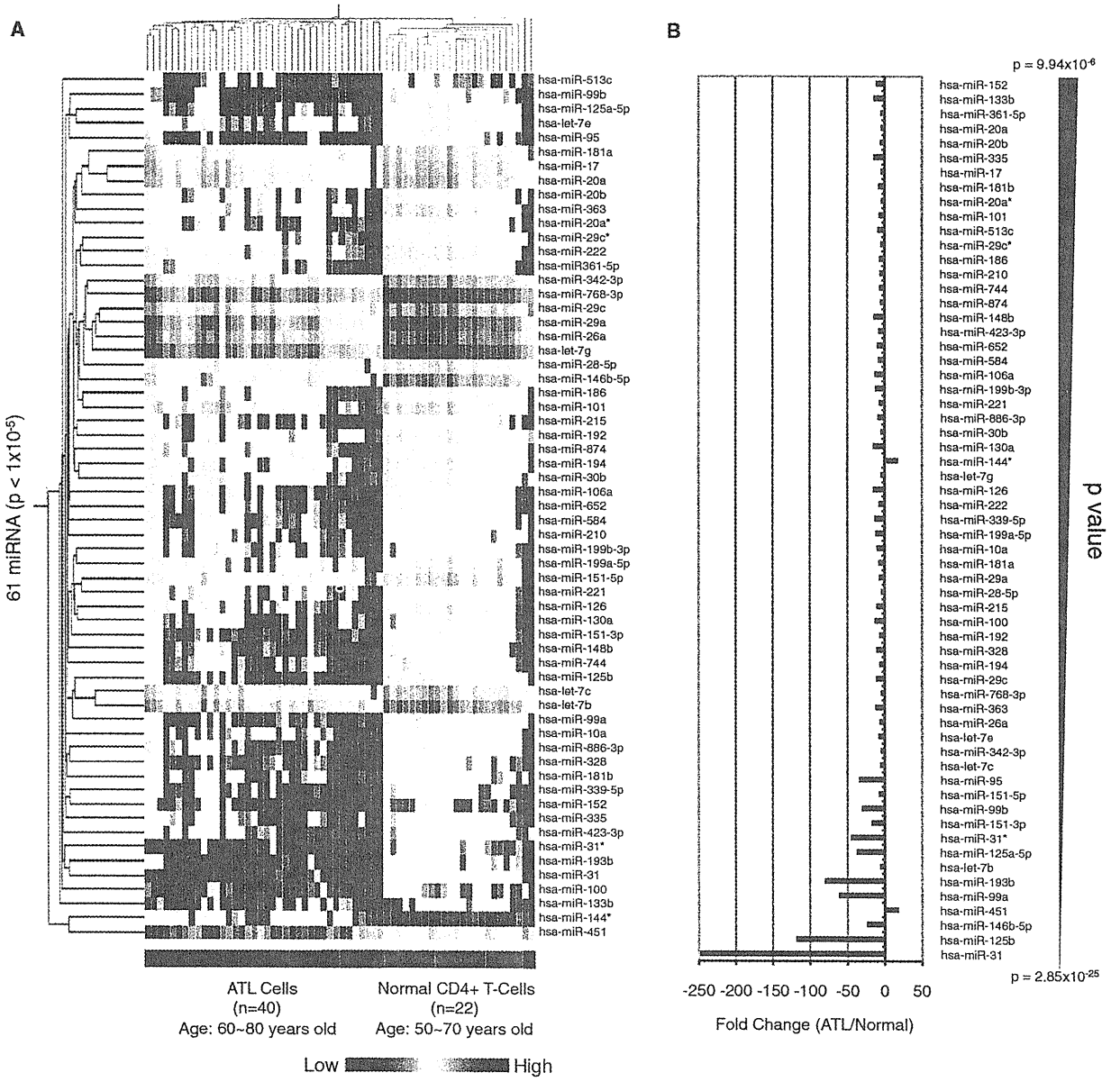

Figure 1. Global Profiling of Cellular miRNA on Primary ATL Cells

(A) Two-dimensional hierarchical clustering analysis and Pearson correlation as similarity measure on the miRNAs expressed at significantly different levels between the ATL (n = 40) and the control (n = 22) groups. Sixty-one miRNAs were identified ($p < 1 \times 10^{-5}$) and by filtering on more than 5-fold changes. A vertical branch shows the expression pattern of the selected miRNAs in each individual.

(B) Fold changes in the 61 miRNAs between ATL and Normal ($p < 10^{-5}$, fold change >5-fold). Selected miRNAs are arranged according to p values. See also Table S1.

UTRWT, or NIK-3′ UTRMu1 and tested their expressions in 293T cells. Results demonstrated that expression of NIK-3′ UTRWT was inhibited by simultaneous introduction of miR-31 (Figure 2E). miR-31 inhibition inversely rescued the NIK level, revealing that the cellular miR-31 level negatively affected that of the NIK protein through its 3′ UTR sequence. These lines of evidence collectively demonstrated that miR-31 recognizes and regulates *NIK* mRNA through specific binding to its 3′ UTR.

Transient introduction of the miR-31 precursor in TL-Om1 cells, which were established from an ATL patient, resulted in downregulation of NIK at the mRNA and protein levels, associated with downregulation of the phospho-IKKα/β level and NF-κB activity (Figures S1F and S1G). In contrast, miR-31 inhibition resulted in accumulation of NIK mRNA and protein in HeLa cells (Figure 2F). Manipulation of the miR-31 level clearly indicated that the miR-31 level negatively correlates with cellular

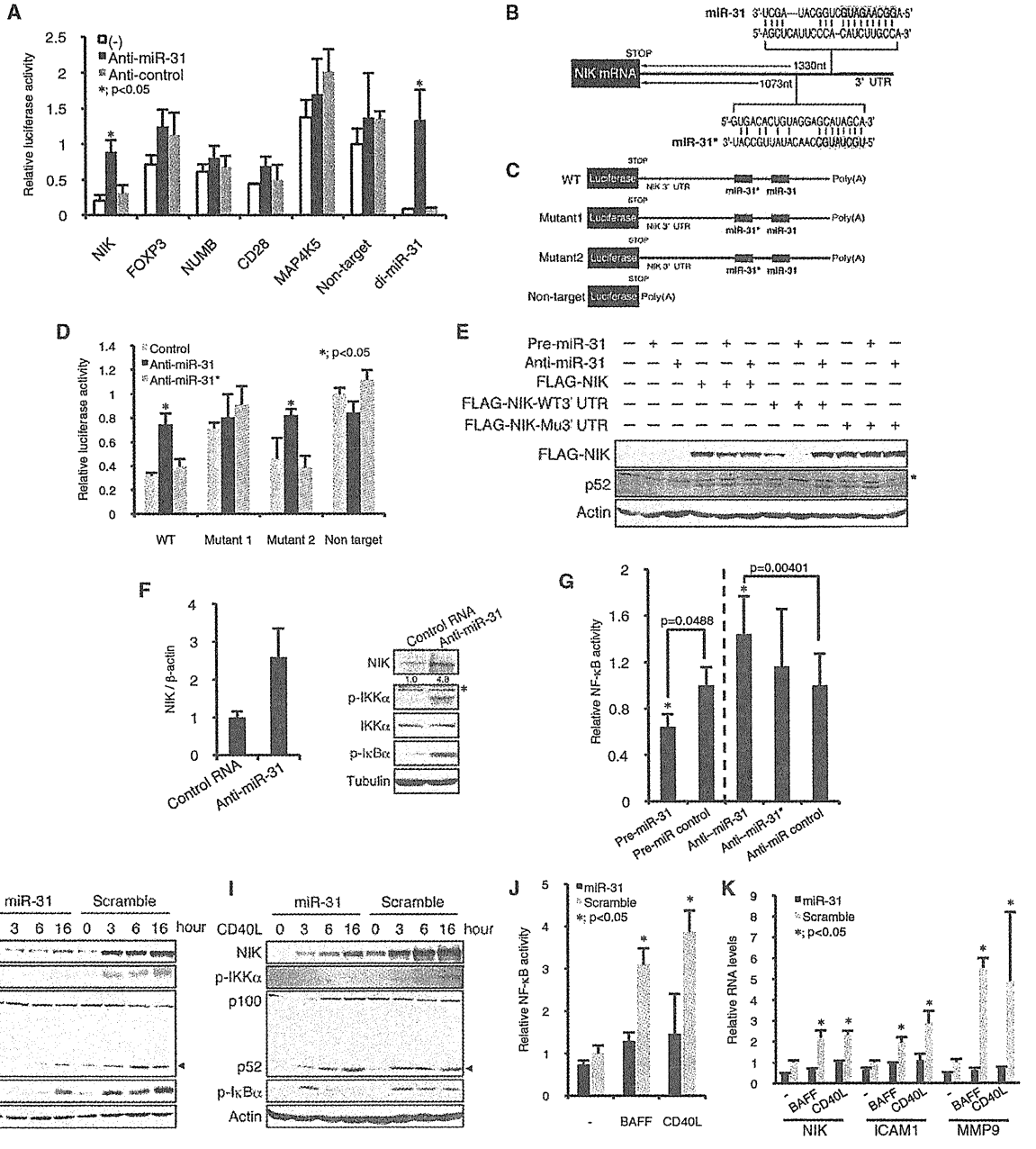

Figure 2. miR-31 Is a Negative Regulator of NF-κB Pathway by Inhibiting NIK Expression

(A) Reporter-based miR-31's target gene screening. A series of 3′ UTR-luciferase reporters was transfected in HeLa cells together with or without miR-31 specific inhibitory RNA (Anti-miR-31) or control RNA (Anti-control). Relative values of Dual-luciferase assay are presented. "Non-target" represents reporter without any 3′ UTR. "di-miR-31" reporter contains two perfect match sequences. The data are presented as mean ± SD of three independent experiments.

(B) Schematic of miR-31 target sites in the *NIK* 3′ UTR.

(C) Mutation-induced reporters. Red box stands for mutated target region (see Figure S1C).

(D) miR-31 negatively regulates *NIK* 3′ UTR analyzed by reporter assay (n = 4, mean ± SD). Luciferase activities of reporter series were tested in a presence or absence of miR-31 inhibitor.

(E) FLAG-tagged NIK protein is negatively regulated through its 3′ UTR and miR-31 binding. Plasmid vectors and miR-31 precursor or miR-31 inhibitor are cotransfected in 293T cells. Western blots showed levels of NIK and endogenous p52. Asterisk indicates nonspecific bands.

(F) NIK mRNA (left) and protein (right) levels in HeLa cells measured by quantitative RT-PCR (n = 3, mean ± SD) and western blotting, respectively. Treatment of miR-31 inhibitor resulted in NIK accumulation. Result of densitometry is shown in the bottom panel. Asterisk indicates nonspecific bands.

(G) Cellular NF-κB activity in HeLa cells (n = 5, mean ± SD) in a presence or absence of miR-31 precursor or inhibitor.

NF-κB activity (Figure 2G). Furthermore, enforced miR-31 expression in B cells attenuated both BAFF and CD40L-mediated NIK accumulation and the subsequent NF-κB signaling (Figures 2H–2K). Consistent with previous reports (Ramakrishnan et al., 2004; Zarnegar et al., 2008b), we also found decreased levels of IκBα phosphorylation. On the other hand, TNF-α-triggered canonical NF-κB activation was not affected by miR-31 in Jurkat cells (Figures S1H–S1K). These results collectively show that miR-31 inhibits the basal and receptor-initiated activities of noncanonical NF-κB pathway. With genetic evidence and an experimental approach, we further demonstrated that the function of miR-31 is well conserved among several classes of species (Figures S1L–S1O). Taking together all these results, miR-31, which is almost completely absent in primary ATL cells, appears to play a critical role in negative regulation of the NF-κB pathway by manipulating the expression of NIK.

miR-31 Suppresses ATL Cell Growth and Promotes Apoptosis by Inhibiting NF-κB

Although it was documented that abnormal NIK accumulation in ATL cells acts as a constitutive activator of the NF-κB pathway, the mechanism underlying overproduction of NIK remains to be elucidated. The results described in the previous section indicated that the amount of miR-31 is linked to the level of NIK, and we therefore speculated that downregulation of miR-31 expression is at least partially responsible for the constitutive activation of NF-κB in ATL cells. Quantitative RT-PCR revealed that *NIK* mRNA levels were negatively correlated with miR-31 levels in primary ATL cell samples (Figure 3A). To investigate the functional roles of NIK and miR-31, we established TL-Om1 cells stably expressing the miR-31 or NIK specific shRNA (shNIK) by retroviral vectors. RT-PCR and western blots showed that expression of miR-31 or shNIK reduced NIK at mRNA and protein levels as well as the levels of phospho-IKKα/β, p52, and IκBα (Figures 3B and 3C). Decreased levels of nuclear RelA and RelB are considered to represent repressed activities of the canonical and noncanonical NF-κB pathways, respectively (Figure 3D). EMSA and NF-κB reporter assays also revealed the repressive function of miR-31 and shNIK on the NF-κB activity (Figures 3E and 3F; Figures S2A, S2B, S5B, and S5C). Re-expression of NIK led to NF-κB activation that was inhibited by miR-31, suggesting a reciprocal relationship between the level of miR-31 and that of NIK.

We and others previously showed that constitutive NF-κB activation is a strong driver of ATL proliferation and prosurvival properties. Here, we examined the effects of miR-31 loss on ATL cell growth. We found that TL-Om1 cells expressing miR-31 or shNIK showed a significant attenuation of cell proliferation compared with control cells. In addition, serum starvation experiments showed greater sensitivity to induced cell death in NIK-repressed cells (Figure 3G). miR-31 expression showed the same phenotypic results in other ATL-derived cell lines (Figures S2C, S2D, and S5E). Jurkat cells do not have significant basal activity of NF-κB, and showed no significant difference in cell growth with or without induced expression of miR-31 (Figure S2E).

Next, we hypothesized that miR-31-mediated NF-κB modulation may affect cellular apoptosis, because numerous studies have demonstrated that NF-κB activation is a strong antiapoptotic factor in ATL and other cancer cells. We found that repression of NIK by miR-31 or shNIK resulted in downregulation of a subset of genes involved in resistance to apoptosis such as BCL-XL, XIAP, and FLIP (Figure 3H), suggesting that miR-31 has a role in proapoptosis through inhibition of NF-κB activity. To assess the biological function of miR-31 in apoptosis signals, we utilized a lentivirus gene transfer system for cell lines and freshly isolated tumor cells. The lentivirus vector is competent to infect nondividing cells and the infected cells can be monitored by the fluorescence of Venus. We found that lentivirus-mediated miR-31 expression promoted basal and Fas-directed apoptosis in TL-Om1 cells (Figure 3I). Venus-negative population showed no significant changes, demonstrating the specificity of miR-31 activity. To confirm the relationship among miR-31, NIK, and NF-κB signaling, we also prepared another retroviral vector encoding NIK without its 3′ UTR sequence. As results, re-expression of NIK reversed the miR-31-mediated apoptosis. In addition, miR-31 expression led to caspase 3 activation (Figure 3J). Collectively, these findings indicate that miR-31 mediates apoptosis through repression of NIK in ATL cell lines.

Tumor cells from ATL patients primarily represent the malignant characteristics. In fact, miR-31 loss is found from patient samples (Figures 1 and 3A). To demonstrate the responsibility of miR-31 for tumor cell survival, we tested whether lentivirus-mediated miR-31 expression has a killing effect against tumor cells. After establishment of lentivirus infection, the apoptotic cells were determined by flow cytometry. The results revealed that expression of miR-31 facilitated tumor cell death. Since NIK repression by shRNA lentivirus also showed a strong killing effect, NIK and NF-κB activity are suggested as crucial players for survival in ATL tumor cells (Figure 3K). Strong toxicities were not observed in normal resting lymphocytes that express low levels of NIK. Taken together, these lines of experimental evidence, including data from cell lines and primary ATL cells, definitively support two notions that (1) miR-31 acts as a tumor suppressor in T cells, and (2) NIK-regulated NF-κB has pivotal importance in cancer cell survival.

Loss of miR-31 Occurs in T Cells with Genetic and Epigenetic Abnormalities

The results described above together with previous publications indicate that regulation of miR-31 expression has profound impacts on multiple functions in human tumors as well as in normal cells. However, little is known about the regulatory mechanism of miR-31 expression. The human gene that encodes miR-31, *hsa-miR-31*, is located at 9p21.3, which is

(H–K) miR-31 attenuates signal-dependent NF-κB activation in B cells. (H and I) BJAB cells expressing miR-31 or control RNA were treated with BAFF (0.2 μg/ml) or CD40L (0.5 μg/ml) for indicated time periods. The protein levels of NIK, phospho-IKKα/β, p100/p52 (arrowheads indicate active p52), and phospho-IκBα were shown. Actin was detected as control. (J) NF-κB activity (n = 5, mean ± SD) evaluated by NF-κB-luciferase reporter assay at 24 hr after cytokine treatments. (K) NF-κB-dependent gene expressions were inhibited by miR-31 (n = 3, mean ± SD). See also Table S2 and Figure S1.

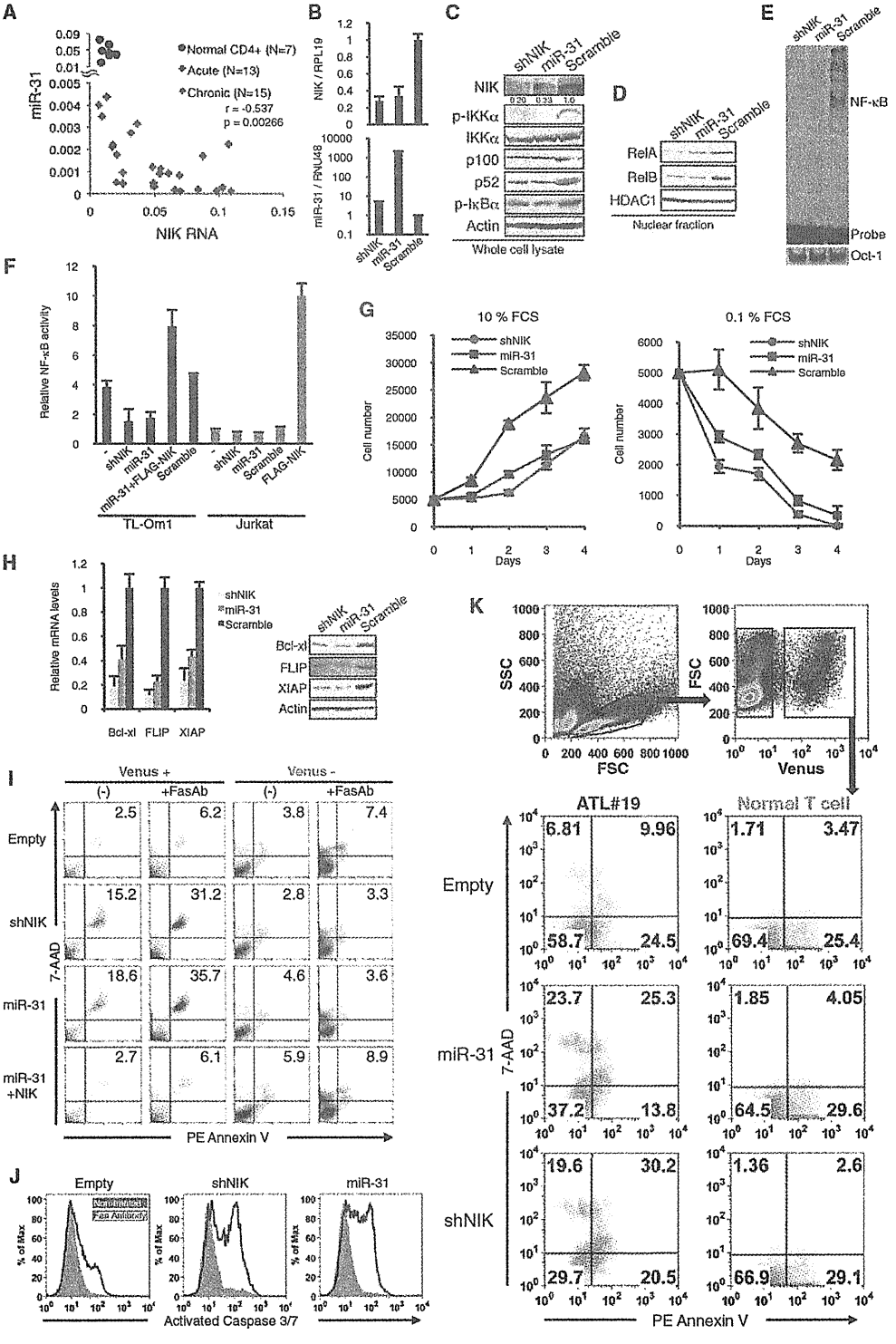

Figure 3. Loss of miR-31 Is Responsible for Constitutive NF-κB Activation, Abnormal Cell Growth, and Resistance to Apoptotic Cell Death in ATL Cells

(A) Expression levels of miR-31 and *NIK* in individual ATL patients and normal controls using data set obtained by quantitative RT-PCR. Pearson's correlation coefficient within ATL samples was described in the graph.

adjacent to clusters of the *CDKN2* and *IFNA* families, and is a well-known hotspot of genomic loss in several types of human cancers. We performed genome-wide scans of genetic lesions in 168 ATL samples and demonstrated that 21 ATL cases (12.5%) had genomic deletion of 9p21.3 containing the *hsa-miR-31* coding region (Figure 4A; Figure S3A). All of these cases also have genomic defect in *CDKN2A* region. A major proportion of ATL cases that are without genetic deletion and somatic mutation in the *hsa-miR-31* region showed remarkable loss of miR-31 expression (Figure 4B). Detailed expression profiling revealed drastic downregulation of *Pri-miR-31* transcription in the primary ATL cells (Figure 4C). There was a strong correlation between the levels of mature miR-31 and primary transcript ($r = 0.9414$, $p = 5.45 \times 10^{-8}$). *hsa-miR-31* is located in intronic region of *LOC554202* gene. However, *LOC554202* mRNA levels were very low in primary T cells and there was no significant difference between ATL and normal cells, strongly suggesting that loss of miR-31 expression is due to specific transcriptional suppression in ATL cells. Using computational analysis, we identified a putative TATA box and transcriptional start site (TSS) 2500 bp upstream of the miR-31 coding region (Figure 4D). Although no CpG islands were found in this region, we unexpectedly discovered an assembly of YY1-binding motifs upstream of the miR-31 region in human and mouse (Figure 4D; Figure S3C). YY1 is a pivotal transcription factor and a recruitor of the Polycomb repressive complex (PRC) (Simon and Kingston, 2009). Convergence of the YY1 binding sequence, especially the repressive motif (Figure S3D), seems to be evolutionarily conserved, suggesting that YY1 is important in the regulation of miR-31 transcription. We further performed chromatin immunoprecipitation (ChIP) to evaluate repressive histone hallmarks, including di- and trimethylated H3K9 (H3K9me2 and H3K9me3) and trimethylated H3K27 (H3K27me3). The results showed higher levels of methylation at H3K9 and H3K27 in a broad area containing the miR-31 coding region (Figure 4E). As shown in Figures S3E–S3G, there was an inverse correlation between the levels of miR-31 expression and repressive histone methylation. These data allowed us to hypothesize that histone methylation, especially that of Polycomb family-dependent H3K27me3, may contribute to miR-31 repression. To confirm our hypothesis, we performed a YY1 knockdown experiment using a specific shRNA (Figures 4F–4I). As expected, knockdown of YY1 led to an increase in the levels of *Pri-miR-31* and mature miR-31 (Figures 4F and 4G). Furthermore, ChIP assays showed that YY1 occupied the miR-31 region, especially in the upstream region of TSS, where there is an array of YY1 binding sites (Figures 4D and 4H). The results also demonstrated that decreased occupancy of YY1 and concomitant derecruitment of EZH2, a key component of PRC2, were induced by YY1 knockdown, indicating involvement of EZH2 in the repressive complex recruited to the miR-31 region (Figures 4H and 4I; Figure S3H). These results collectively suggest that YY1 regulates PRC2 localization and initiates miR-31 suppression. Indeed, we found significant escalation of methylated histone H3K9 and H3K27 at the miR-31 locus of peripheral blood lymphocytes of ATL patients (Figure 4J), indicating that aberrant abundance of suppressive histone methylation may be responsible for the loss of miR-31 in the primary ATL cells.

Overexpression of PRC2 Components Leads to miR-31 Repression

Given that Polycomb-mediated repressiveness affects miR-31 level, our findings imply that the amount of EZH2 is related to miR-31 expression (Figure 4I; Figures S3G and S4A). We found a significantly upregulated expression of PRC2 components, especially EZH2 and SUZ12, in the primary ATL cells (Figures 5A and 5B; Table S3). Quantitative RT-PCR revealed that miR-31 levels inversely correlated with both *EZH2* and *SUZ12*, respectively (Figure 5C). miR-101 and miR-26a, which are putative negative regulators of EZH2, seem to be associated with this relationship in ATL cells (Figures S4B–S4E). To further confirm our hypothetical mechanism linking the epigenetic machinery and miR-31 expression, we performed a "loss-of-PRC2-function" assay. Retroviral delivery of shSUZ12 and shEZH2 in the ATL cell lines resulted in a great increase in the levels of *Pri-miR-31* and its mature form (Figure 5D; Figure S4F). Knockdown of PRC2 induced histone demethylation at H3K27 in the miR-31 region, which is concomitant with the decrease in H3K9me3 levels, EZH2 occupancy, and HDAC1 recruitment (Figure 5E), suggesting that this multimeric complex leads to a completely closed chromatin architecture as a result of histone modifications in the miR-31 genomic region.

To further examine whether the proposed mechanism holds true in other human cancers, we analyzed a couple of carcinoma cell lines, including HeLa cells and nonmetastatic and metastatic breast carcinoma cell lines, MCF7 and MDA-MB-453 cells, respectively. qRT-PCR revealed that expression of *EZH2* and *SUZ12* inversely correlated with miR-31 levels (Figure S4G).

(B) miR-31 restoration by retroviral vector inhibits *NIK* RNA accumulation in TL-Om1 cells. The results of *NIK* and mature miR-31 quantifications are shown (n = 3, mean ± SD).
(C) miR-31 or shNIK expression downregulates NIK protein expression and inhibits downstream pathway of noncanonical NF-κB in TL-Om1 cells.
(D) Reduced nuclear translocation of RelA and RelB proteins in miR-31- or shNIK-expressing TL-Om1 cells.
(E) miR-31-dependent downregulation of NF-κB activity in TL-Om1 cells examined by EMSA.
(F) NF-κB-luciferase reporter assays (n = 5, mean ± SD). FLAG-NIK plasmid was transiently introduced 48 hr prior to the assay.
(G) miR-31 level is relevant to proliferation of ATL cells. Cell proliferation curve of TL-Om1 cells were evaluated in two FCS conditions (n = 3, mean ± SD).
(H) Apoptosis-related gene expression in TL-Om1 cells analyzed by qRT-PCR (n = 3, mean ± SD) and western blots.
(I) Lentivirus-mediated NIK depletion promotes basal and Fas antibody-mediated apoptosis. Venus-positive population represented lentivirus-infected cells. Apoptotic cells were determined by PE-Annexin V / 7-AAD stainings (n = 4). Representative FACS analyses are shown.
(J) miR-31 activates Caspase 3/7 determined by FACS (n = 3).
(K) miR-31 expression and NIK depletion induce tumor cell death. Primary tumor cell from ATL patient and healthy CD3+ T cells were infected with lentivirus and analyzed by FACS. The apoptotic cells were defined by sequential gating beginning with FSC-SSC to select intact lymphocytes, subgating on the Venus-positive population, and calculating the PE-Annexin V and 7-AAD profilings. Representative result is shown and summarized data are presented in Figure 6J. See also Figure S2.

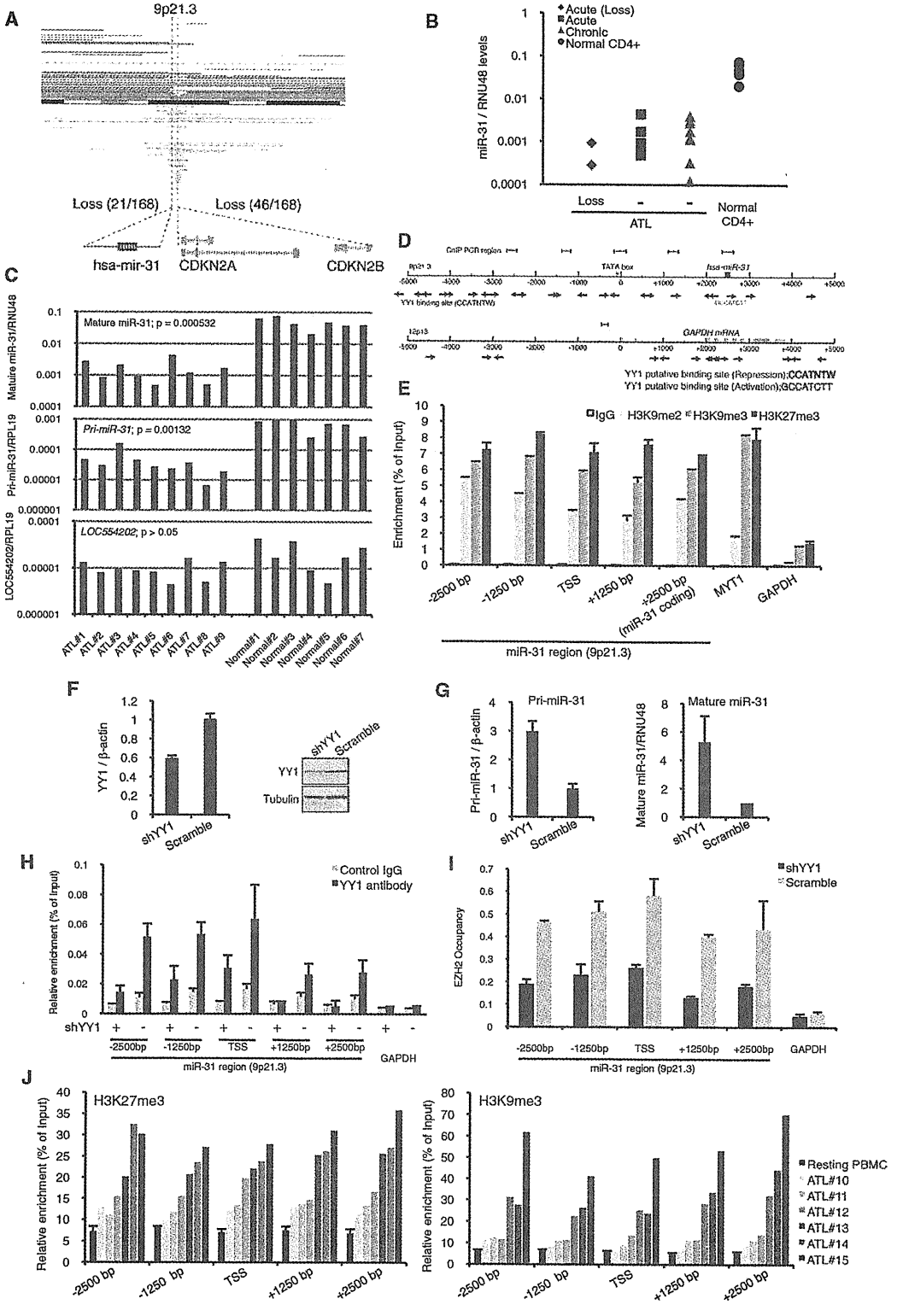
A
9p21.3
Loss (21/168)
Loss (46/168)
hsa-mir-31
CDKN2A
CDKN2B
B
Acute (Loss)
Acute
Chronic
Normal CD4+
miR-31 / RNU48 levels
Loss
ATL
Normal CD4+
C
Mature miR-31; p = 0.000532
Pri-miR-31; p = 0.00132
LOC554202; p > 0.05
Mature miR-31/RNU48
Pri-miR-31/RPL19
LOC554202/RPL19
ATL#1 ATL#2 ATL#3 ATL#4 ATL#5 ATL#6 ATL#7 ATL#8 ATL#9
Normal#1 Normal#2 Normal#3 Normal#4 Normal#5 Normal#6 Normal#7
D
ChIP PCR region
TATA box
hsa-miR-31
GAPDH mRNA
YY1 putative binding site (Repression);CCATNTW
YY1 putative binding site (Activation);GCCATCTT
E
IgG H3K9me2 H3K9me3 H3K27me3
Enrichment (% of Input)
-2500 bp
-1250 bp
TSS
+1250 bp
+2500 bp (miR-31 coding)
MYT1
GAPDH
miR-31 region (9p21.3)
F
YY1 / β-actin
shYY1
Scramble
YY1
Tubulin
G
Pri-miR-31
Mature miR-31
Pri-miR-31 / β-actin
Mature miR-31/RNU48
H
Control IgG
YY1 antibody
Relative enrichment (% of Input)
shYY1
-2500bp -1250bp TSS +1250bp +2500bp GAPDH
miR-31 region (9p21.3)
I
shYY1
Scramble
EZH2 Occupancy
-2500bp -1250bp TSS +1250bp +2500bp GAPDH
miR-31 region (9p21.3)
J
H3K27me3
H3K9me3
Relative enrichment (% of Input)
-2500 bp -1250 bp TSS +1250 bp +2500 bp
Resting PBMC
ATL#10
ATL#11
ATL#12
ATL#13
ATL#14
ATL#15

ChIP assays detected higher levels of trimethylated H3K27 and EZH2 occupancy in cells showing lower expression levels of miR-31 (Figure S4H). Furthermore, knockdown of EZH2 or SUZ12 restored miR-31 transcription in MDA-MB-453 and MCF7 cells (Figures 5F and 5G; Figure S4K, respectively), which are consistent with the results obtained with ATL cells. These results indicate a link between Polycomb-mediated epigenetic regulation and miR-31 transcription in ATL and breast cancer cell lines.

Polycomb Group Regulates NF-κB Pathway by Controlling miR-31 Expression

Based on our findings, we considered an aspect of the biological communication between epigenetic silencing and the NF-κB pathway through miR-31 regulation. The microarray data sets showed positive correlations between PRC2 components and miR-31 target gene, *NIK* expression (Figure 6A). The results also suggested that these factors tend to show higher levels in the aggressive subtype (acute type) than in the indolent subtypes (chronic and smoldering types), implying that these genes may play important roles in the clinical phenotype and prognosis of ATL. To examine this notion, we performed PRC2 knockdown in ATL cell lines. Western blots of these cells demonstrated decreased levels of NIK, p52, and phospho-IκBα (Figure 6B; Figure S5A), suggesting suppression of both canonical and noncanonical NF-κB cascade and activity (Figure 6C; Figures S5B and S5C). These results are consistent with those of miR-31 overexpression (Figures 3C–3F). Then, we tested whether exogenous manipulation of miR-31 could restore the effect of PRC2 loss. Anti-miR-31 treatment rescued impaired NF-κB activity in PRC2-disrupted cells (Figure 6D). On the other hand, overexpression of EZH2 induced NF-κB activation, which was partially canceled by the introduction of miR-31 precursor (Figure 6E; Figure S5D). These results suggest that Polycomb-mediated miR-31 suppression leads to NF-κB activation. Indeed, knockdown of the PRC2 complex led to reduced levels of cell proliferation and greater sensitivity to serum deprivation in ATL cells (Figure 6F; Figure S5E). In addition, PRC2 disruption showed a reduction in cell migration (Figure S5F).

To gain further insight into this general network, we studied the functions of miR-31 and the PRC2 complex in breast cancer cell lines. NF-κB activity was downregulated by knockdown of PRC2 components in MDA-MB-453 cells (Figure 6G; Figures S5G and S5H), although no significant differences were observed in cell proliferation (data not shown). Repression of NF-κB activity induced by knockdown of PRC2 components was partially restored by treatment with a miR-31 inhibitor, suggesting that PRC2 knockdown-mediated relief of NF-κB repression is at least a part of the result of the miR-31 induction. In addition, knockdown of PRC2 components resulted in a reduced level of receptor-initiated accumulation of NIK in B cells (Figure 6H). Our findings indicate a common molecular mechanism comprising Polycomb-mediated epigenetic regulation, miR-31 expression and the NF-κB signaling pathway.

Regulation of NF-κB by Polycomb family may in turn control the cellular apoptosis responses. We found that lentivirus-mediated EZH2 knockdown led to increased apoptotic sensitivity in TL-Om1 cells (Figure 6I). Additional expression of NIK inhibited the cell death induced by EZH2 knockdown, suggesting the reciprocal relationship between Polycomb and NF-κB cascades. By using primary tumor cells from patient, we tested the killing effect induced by miR-31, NIK knockdown, and EZH2 knockdown (Figure 6J; Figures S5I and S5J). All tested samples showed strong death response, demonstrating that survival of ATL cells was closely associated with miR-31, NIK, and EZH2, all of which show deregulated expression in ATL cells.

By qRT-PCR we finally examined the expression levels of some genes involved in the noncanonical NF-κB pathway. As shown in Figure 6K, the results clearly demonstrated higher expression levels of positive regulators such as *NIK*, *CD40*, and *LTBR*, and lower expression levels of the negative regulators such as *BIRC2/3* (cIAP1/2), which are involved in proteasomal degradation of NIK (Zarnegar et al., 2008a). These observations are in line with a previous report on Multiple Myeloma cells (Annunziata et al., 2007). In addition to these data, we obtained convincing evidence for a molecular aspect of NIK accumulation in ATL cells. Polycomb-dependent epigenetic gene silencing may be associated with miR-31 loss, followed by NF-κB activation and other signaling pathways (Figure 7).

DISCUSSION

Constitutive activation of NF-κB contributes to abnormal proliferation and inhibition of apoptotic cell death in cancer cells,

Figure 4. Genetic and Epigenetic Abnormalities Cause miR-31 Loss in ATL Cells

(A) Genomic loss of chromosome 9p21.3 in primary ATL cells. Copy number analyses revealed tumor-associated deletion of miR-31 region (21/168) and *CDKN2* region (46/168). Recurrent genetic changes are depicted by horizontal lines based on CNAG output of the SNP array analysis.

(B) miR-31 expression in various sample sets. Expression levels were evaluated by real-time PCR.

Loss, samples with genomic loss of the miR-31 region; (–) samples without genomic loss of the miR-31 region.

(C) PCR-based miR-31 quantifications in primary ATL samples. ATL samples without genetic loss in miR-31 region (n = 9, Figure S3B), and normal CD4+ T cells (n = 7) were tested. p values (ATL versus normal) are shown.

(D) YY1 binding motif cluster around transcriptional start site (TSS) of miR-31 region. Arrows represent positions of the motifs. Regions of PCR amplification for ChIP assay are shown.

(E) Repression-associated histone methylation in miR-31 region determined by ChIP assay (n = 3, mean ± SD). The results of relative enrichment against input control are presented and distance from miR-31 TSS is described. *MYT1* and *GAPDH* promoters are as positive or negative controls, respectively.

(F–I) YY1-dependent EZH2 occupancy in miR-31 locus. (F) YY1 knockdown in TL-Om1 cells. qRT-PCR (left, n = 3, mean ± SD) and western blotting (right) showed decreased YY1 level. (G) YY1 knockdown led to both primary and mature miR-31 restoration in TL-Om1 cells (n = 3, mean ± SD). (H) YY1 occupancy in miR-31 region analyzed by ChIP (n = 3, mean ± SD). YY1 occupancy in miR-31 locus was reduced by YY1 knockdown. (I) EZH2 occupancy in miR-31 region analyzed by ChIP (n = 3, mean ± SD). YY1 knockdown inhibited EZH2 recruitment in miR-31 region.

(J) Aberrant accumulation of repression-associated histone methylations widely in miR-31 region of primary ATL cells. PBMCs freshly isolated from ATL patients (n = 6) were analyzed by ChIP assay. PBMC from healthy adults were used for normal controls. See also Figure S3.

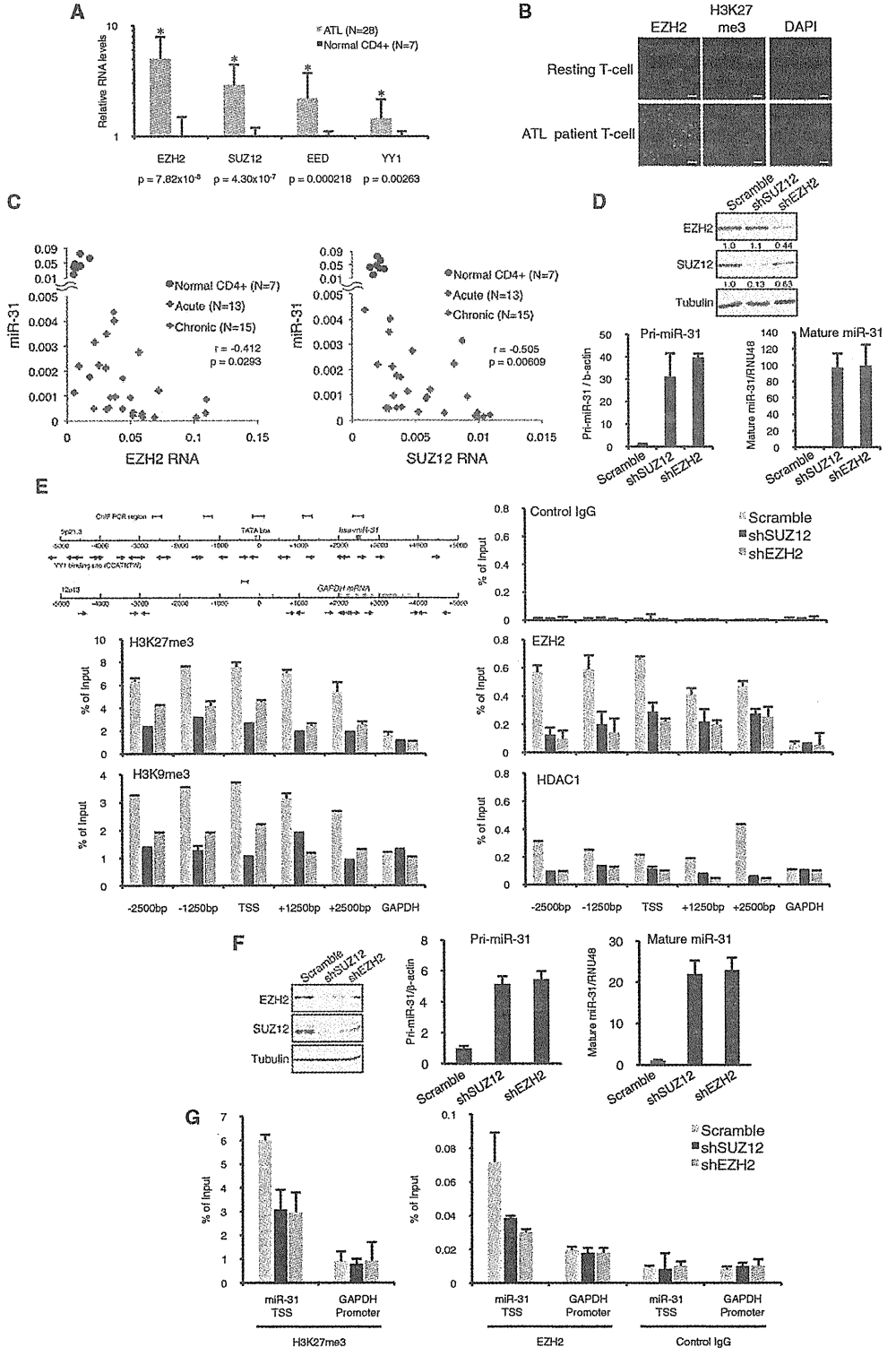
A
Relative RNA levels
ATL (N=28)
Normal CD4+ (N=7)
EZH2
SUZ12
EED
YY1
p = 7.82x10-8
p = 4.30x10-7
p = 0.000218
p = 0.00263
B
H3K27 me3
EZH2
DAPI
Resting T-cell
ATL patient T-cell
C
miR-31
Normal CD4+ (N=7)
Acute (N=13)
Chronic (N=15)
r = -0.412
p = 0.0293
EZH2 RNA
r = -0.505
p = 0.00609
SUZ12 RNA
D
Scramble
shSUZ12
shEZH2
EZH2
SUZ12
Tubulin
Pri-miR-31
Pri-miR-31 / b-actin
Mature miR-31
Mature miR-31/RNU48
E
Control IgG
Scramble
shSUZ12
shEZH2
% of Input
H3K27me3
EZH2
H3K9me3
HDAC1
-2500bp
-1250bp
TSS
+1250bp
+2500bp
GAPDH
F
Scramble
shSUZ12
shEZH2
EZH2
SUZ12
Tubulin
Pri-miR-31
Pri-miR-31/β-actin
Mature miR-31
Mature miR-31/RNU48
G
Scramble
shSUZ12
shEZH2
% of Input
miR-31 TSS
GAPDH Promoter
H3K27me3
EZH2
Control IgG

including ATL, diffuse large B cell lymphoma (DLBCL), Hodgkin lymphoma, breast cancer, prostate cancer and others (Prasad et al., 2010). NF-κB is also essential for various cell functions, including inflammation, innate immunity, and lymphocytic development (Hayden and Ghosh, 2008). Identification of NF-κB determinants will lead to marked progress in understanding molecular pathology.

Our global analyses demonstrated an interesting miRNA expression signature as well as an aberrant mRNA expression profile, which may be associated with leukemogenesis in the primary ATL cells (Figures 1 and 6A). We revealed downregulation of tumor-suppressive miRNA including Let-7 family, miR-125b, and miR-146b, which can contribute to aberrant tumor cell signaling. Recent studies have suggested unique expression profiles of miRNAs in ATL (Yeung et al., 2008; Bellon et al., 2009), but loss of miR-31 has not been focused. Cellular amount of miRNAs may be susceptible to various environments such as transcriptional activity, maturation processing, and also epigenetic regulation. The end results appear to be affected by methodology employed and conditions and types of samples used. Our integrated expression profiling of primary ATL cells are based on a significantly larger number of samples and fruitfully provides intriguing information that may be useful in improving the understanding of T cell biology as well as in the identification of biomarkers for diagnosis.

Pleiotropy of miR-31 was first reported by Valastyan et al. (2009). The authors elegantly demonstrated the function of miR-31 in vivo and also identified several target genes that contribute to cell migration and invasiveness. In the present study, we focused on the functional significance of miR-31 in the regulation of NF-κB signaling that contributes to tumor cell survival.

Overexpression of NIK acts as an oncogenic driver in various cancers. In the present study, NIK was identified as a miR-31 target based on several lines of evidence. First, luciferase-3′ UTR reporter assay showed that *NIK* 3′ UTR sequence has a role for negative regulation (Figure S1B). By combining a specific inhibitor and mutations in miR-31-binding site, we demonstrated that miR-31 recognizes and negatively regulates the *NIK* 3′ UTR (Figures 2A and 2D). Second, by introducing a miR-31 precursor or inhibitor, we showed that amount of miR-31 inversely correlates with levels of NIK expression and downstream signaling (Figures 2E–2K). Third, genetic evidence indicated strong base pairing and biological conservation (Bartel, 2009) (Figures S1L–S1O). Our experimental approach illustrated that mmu-miR-31 regulates mouse *Map3k14* gene. Fourth, individual assessments using gene expression data clearly revealed an inverse correlation between the expression levels of miR-31 and *NIK* (Figure 3A). Collectively, we provide definitive evidence for the notion that miR-31 negatively regulates NIK expression and activity.

It is well known that the NIK level directly regulates NF-κB activity in various cell types (Thu and Richmond, 2010). We experimentally showed that miR-31 regulates noncanonical NF-κB activation stimulated by BAFF and CD40L, both of which are major B cell activating cytokines. Since signals from receptors are essential for the development and activity of B cells, the negative role of miR-31 in cytokines-induced NIK accumulation appears to be widely important in the noncanonical regulation of NF-κB in B cells and other cell types (Figures 2H–2K). Again, our findings revealed the role of NIK in the regulation of canonical NF-κB pathway. Strict regulation of NIK appears to be closely associated with the fate of lymphocytes.

The level of miR-31 was drastically suppressed in all tested primary ATL cells, and its magnitude is greater than that which has been reported in other cancers. Our results demonstrated a profound downregulation of miR-31 (fold change, 0.00403; Figure 1B) in all ATL cases, suggesting that miR-31 loss is a prerequisite for ATL development. Restoration of miR-31-repressed NF-κB activity in ATL cells, resulting in impairment of the proliferative index and apoptosis resistance (Figure 3). Furthermore, our results demonstrate that inhibition of NF-κB promotes tumor cell death in cell lines and also primary tumor cells from ATL patients (Figures 3 and 6), which are consistent with our previous observation (Watanabe et al., 2005). Since it is highly possible that miR-31 and relevant factors are pivotal in cancers, their expressions would have a great importance in view of biomarkers for the aberrant signaling and clinical outcomes.

By studying clinical samples and in vitro and ex vivo models, we obtained several biologically interesting results. First, we identified the Polycomb protein complex as a strong suppressor of miR-31. Generally, the Polycomb group constitutes a multimeric complex that negatively controls a large number of genes involved in cellular development, reproduction, and stemness (Sparmann and van Lohuizen et al., 2006). However, the key molecules involved in cancer development, progression, and prognosis are not yet fully understood. In breast and prostate cancers, oncogenic functions of EZH2 and NF-κB activation were reported independently (Kleer et al., 2003; Varambally et al., 2002; Suh and Rabson, 2004). Interestingly, these tumors show low miR-31 levels (Valastyan et al., 2009; Schaefer et al., 2010). Recently, Min et al. (2010) reported that EZH2 activates NF-κB by silencing the DAB2IP gene in prostate cancer cells.

Figure 5. Amount of PRC2 Components Epigenetically Links to miR-31 Expression in T Cells and Epithelial Cells

(A) Overexpression of PRC2 components in primary ATL cells measured by qRT-PCR (ATL, n = 28; normal, n = 7; mean ± SD). These results were supported by the data of gene expression microarray (Table S3).

(B) Escalation of EZH2 protein and trimethylated H3K27 levels in primary ATL cells illustrated by immunocytostaining (n = 4, a representative result is shown). Resting T cells were as normal control. Scale bars = 20 μm.

(C) Statistical correlation among the levels of miR-31, *EZH2*, and *SUZ12* in individual ATL samples. Correlation coefficients within ATL samples are shown in the graphs.

(D and E) Loss of PCR2 function causes chromatin rearrangement and miR-31 upregulation. (D) TL-Om1 cells expressing shSUZ12, shEZH2, and scrambled RNA were established by retroviral vector. The levels of EZH2, SUZ12, *Pri-miR-31*, and mature miR-31 were measured by western blotting and qRT-PCR (n = 3, mean ± SD). (E) Results of ChIP assays with indicated antibodies (n = 3, mean ± SD). Amounts of immunoprecipitated DNA were analyzed by region-specific PCR. *GAPDH* promoter served as a region control.

(F and G) Knockdown of Polycomb family proteins in MDA-MB-453 cells. (F) EZH2 and SUZ12 are shown by western blot. miR-31 level was examined by qRT-PCR (n = 3, mean ± SD). (G) Histone methylation and EZH2 occupancy evaluated by ChIP assay (n = 3, mean ± SD). See also Table S3 and Figure S4.

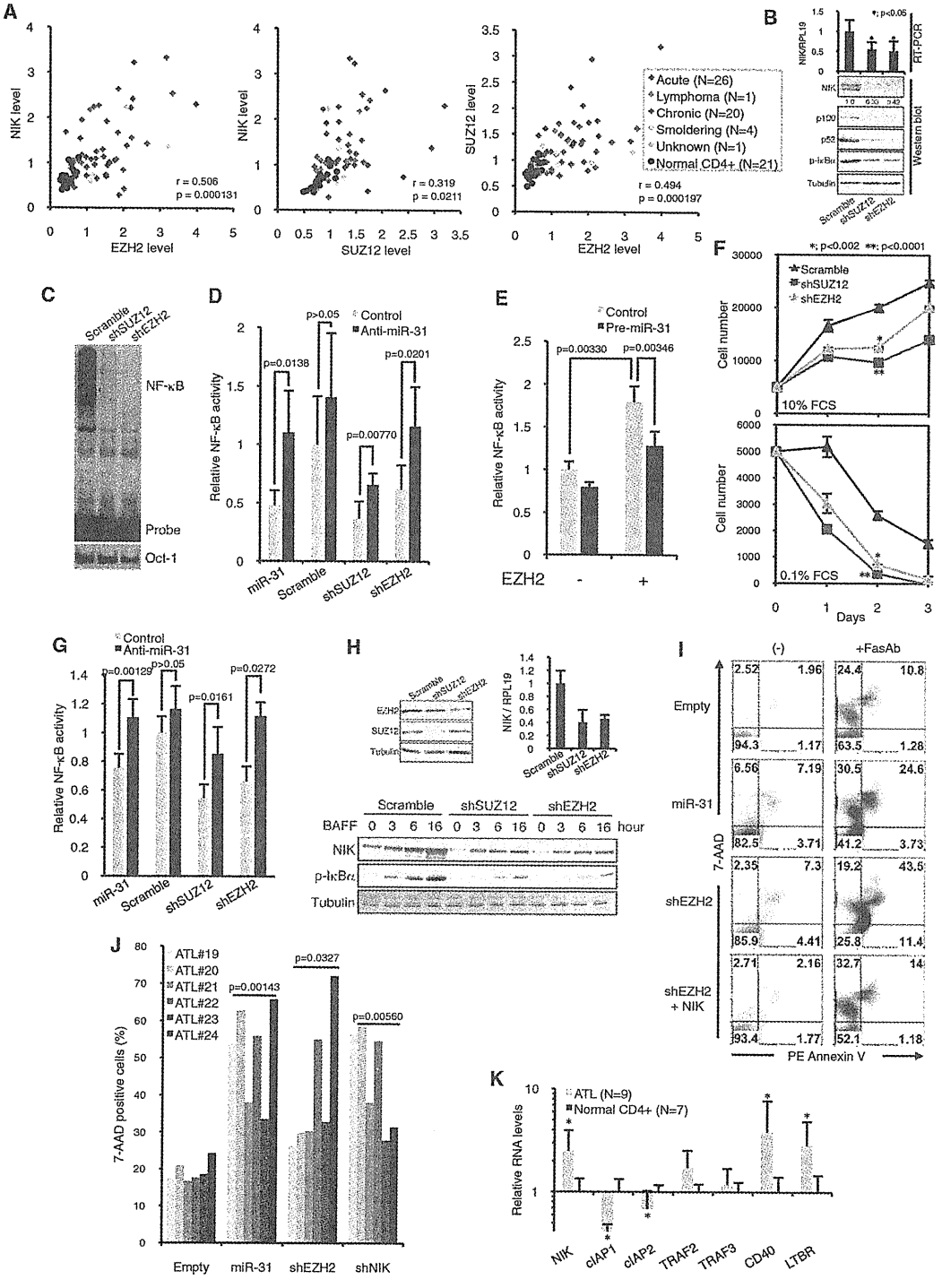

Figure 6. Epigenetic Change Driven by Polycomb Group Mediates NF-κB Signaling through miR-31 Regulation

(A) Reciprocal relationship of mRNA expression between *NIK* and Polycomb group in primary samples. Pearson's correlation coefficients among ATL samples are shown.

(B) PRC2 knockdown negatively affects NF-κB signaling in TL-Om1 cells. After establishment of PRC2 knockdown, the levels of *NIK* RNA (n = 4, mean ± SD) and proteins of NIK, p52/p100, and phospho-IκBα were examined.

(C) Downregulation of NF-κB activity in PRC2-disrupted cells detected by EMSA.

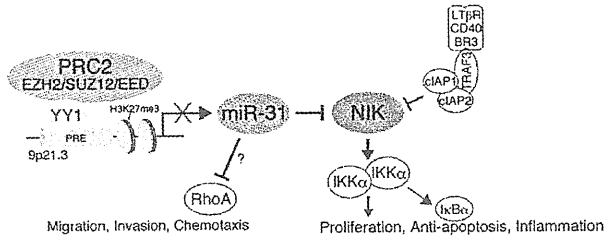

Figure 7. Proposed Model for ATL and Other Tumor Cells
Polycomb repressive factors are linked to NIK-dependent NF-κB activation via miR-31 regulation.

In the present study, we found that the Polycomb group regulates miR-31 expression and that elevated expression of EZH2 leads to NF-κB activation via NIK-miR-31 regulation in ATL and breast cancer cells (Figure 6). We also showed that restoration of miR-31 partially impaired Polycomb-mediated NF-κB operation (Figures 6D, 6E, and 6G), suggesting that miR-31 is involved in this relationship. Furthermore, a connection between NIK and PRC2 was observed in B cells (Figure 6H). Polycomb group proteins are essential in lymphocyte development and activation (Su et al., 2003, 2005). Further, given the NF-κB is a pivotal transcription regulator in normal and oncogenic functions, practical participations of epigenetic regulators and miR-31 in NF-κB signaling will increase our understanding of the molecular mechanisms of T cell functions. For generalization of the molecular axis in other cancers and normal cells, further study will be needed.

Second, YY1 is a recruiter of PRC2 to the miR-31 region. In humans, the Polycomb response element (PRE) has not been precisely identified. A good candidate for a mammalian recruiter of PRC2 is YY1, the homolog of *D. melanogaster* PHO (Simon and Kingston, 2009). We found an assembly of the YY1 binding motif in the miR-31 locus and demonstrated that YY1 knockdown dislodged EZH2 in this region (Figure 4I), which supports previous findings (Caretti et al., 2004). The detailed mechanism by which YY1 mediates recruitment of the Polycomb family may be important in the context of epigenetic regulation of orchestrated gene expression and T cell functions.

Third, Polycomb family proteins can control miRNA expression in an epigenetic fashion. The amount of PRC2 factors strongly influenced the degree of suppression of miR-31 expression (Figure 5). We speculate that, in addition to controlling the transcription, the Polycomb group can modulate translation via miRNA regulation. Furthermore, miR-101 and miR-26a are known to regulate EZH2 expression (Sander et al., 2008; Varambally et al., 2008), which is supported by our observation (Figure S4C). This signaling circuit will permit multiple gene regulation. Whereas genetic loss at the miR-31 locus is observed in some cases of ATL (Figure 4A), no genetic deletion in the miR-101-1 or miR-101-2 region was detected in ATL, which is not consistent with a previous finding in prostate cancer. Our results also suggested putative association between Let-7 family and EZH2 (Figure S4). Aberrant downregulations of these miRNAs in the primary ATL cells will be the next important questions to be addressed in efforts to improve understanding of the oncogenic signaling network.

By collaborative profiling of miRNA and mRNA expression, we identified a notable relationship between ATL subtypes and a gene cluster that contains miR-31, NIK, EZH2, and SUZ12. This finding suggests that an aberrant gene expression pattern correlates with the malignant phenotype, and this provides important clues about clinical manifestations and may help identify therapeutic targets against ATL cells (Figure 6A). Although HDAC inhibitors did not show effective responses (Figures S4I and S4J), emerging epigenetic drug such an EZH2 inhibitor (Fiskus et al., 2009) may pave a pathway leading to cures for various malignancies that involve constitutive activation of NF-κB.

In summary, we show that genetic and epigenetic loss of miR-31 is responsible for oncogenic NF-κB activation and malignant phenotypes in ATL. This provides evidence for the idea that miR-31 is an important tumor suppressor. An emerging pathway involving an epigenetic process, miR-31, and NF-κB will provide a conceptual advance in epigenetic reprogramming, inflammatory signaling, and oncogenic addiction.

EXPERIMENTAL PROCEDURES

Cell Lines and Primary ATL Cells

The primary peripheral blood mononuclear cells (PBMCs) from ATL patients and healthy volunteers used in the present work were a part of those collected with an informed consent as a collaborative project of the Joint Study on Prognostic Factors of ATL Development (JSPFAD). The project was approved by the Institute of Medical Sciences, the University of Tokyo (IMSUT) Human Genome Research Ethics Committee. Additional ATL clinical samples for copy number analysis were provided by Drs. Y. Yamada, Nagasaki University,

(D) NF-κB activity evaluated by reporter assays in the presence or absence of miR-31 inhibitor (n = 5, mean ± SD). Anti-miR-31 treatment partially rescued the NF-κB activity in PRC2 knockdowned TL-Om1 cells.
(E) Overexpressed EZH2 activates NF-κB via miR-31. Jurkat cells were transfected with an EZH2 plasmid together with miR-31 precursor or control RNA (n = 5, mean ± SD).
(F) PRC2 dysfunction changes TL-Om1 cell proliferation and response to serum starvation. Under conditions of 10% or 0.1% of FCS, cell growth curves were examined (n = 3, mean ± SD). PRC2 downregulation decreased cell growth with statistical significance.
(G) NF-κB activity in PRC2-knockdowned MDA-MB-453 cells in the presence or absence of miR-31 inhibitor were examined (n = 5, mean ± SD).
(H) PRC2 disruption inhibits BAFF-dependent NIK accumulation and IκBα phosphorylation in BJAB cells.
(I) Apoptotic cell death induced by lentivirus-mediated EZH2 knockdown in TL-Om1. Venus-positive populations were analyzed by Annexin V/7-AAD stainings (n = 3) and representative of FACS data are shown.
(J) Summary of primary tumor cell death. Lentivirus-based miR-31 expression, NIK knockdown, and EZH2 knockdown showed killing effects in six primary ATL samples. Statistical significances are shown in the graph. Results of FACS and qRT-PCR are shown in Figures S5I and S5J.
(K) Expression levels of genes involved in noncanonical NF-κB pathway in primary ATL cells (ATL, n = 9; normal, n = 7; mean ± SD). Relative expression levels were tested by qRT-PCR (*$p < 0.05$). See also Figure S5.

and K. Ohshima, Kurume University, where the projects were approved by the Research Ethics Committees of Nagasaki University and Kurume University, respectively. PBMC were isolated by Ficoll separation. ATL cells, primary lymphocytes, and all T cell lines were maintained in RPMI1640 supplemented with 10% of FCS and antibiotics. Clinical information of ATL samples is provided in Table S1.

Expression Analyses

Clinical samples for microarrays were collected by a collaborative study group, JSPFAD (Iwanaga et al., 2010). Gene expression microarray was used 4x44K Whole Human Genome Oligo Microarray (Agilent Technologies) and miRNA microarray was used Human miRNA microarray kit v2 (Agilent Technologies), respectively. Quantitative RT-PCR was performed with SYBRGreen (TAKARA). Mature miRNA assays were purchased from Applied Biosystems.

Copy Number Analyses

Genomic DNA from ATL patients was provided from the material bank of JSPFAD, Nagasaki University, and Kurume University, and was analyzed by Affymetrix GeneChip Human Mapping 250K Nsp Array (Affymetrix). Obtained data were analyzed by CNAG/AsCNAR program (Chen et al., 2008).

Oligonucleotides, Plasmids, and Retrovirus Vectors

All RT-PCR primers and oligonucleotides are described in Supplemental Experimental Procedures. miRNA precursor and inhibitor were from Applied Biosystems. Transfection of small RNA and other plasmid DNA were performed by Lipofectamine2000 (Invitrogen). For miRNA or shRNA expression, retroviral vectors (pSINsi-U6, TAKARA) were used.

3′ UTR-Conjugated miR-31 Reporter Assay

HeLa cells were cotransfected with 3′ UTR-inserted pMIR-REPORT firefly plasmid (Ambion), RSV-Renilla luciferase plasmid, and miRNA inhibitor. The cells were collected at 24 hr posttransfection, and Dual-luciferase reporter assay was performed (Promega).

Analysis of NF-κB Pathway

NF-κB activity was evaluated by EMSA and reporter assays as previously described (Horie et al., 2004). Antibodies for western blots are described in supplemental information. Cell proliferative assay was performed by Cell Counting Kit-8 (Dojindo).

Lentivirus Vectors and Apoptosis Analysis

A lentivirus vector (CS-H1-EVBsd) was provided from RIKEN, BRC, Japan. Lentivirus solution was produced by cotransfection with packaging plasmid (pCAG-HIVgp) and VSV-G- and Rev-expressing plasmid (pCMV-VSV-G-RSV-Rev) into 293FT cells. After infection of lentivirus, the apoptotic cell was evaluated by PE Annexin V / 7-AAD staining (BD PharMingen) and analyzed by FACS Calibur (Becton, Dickinson). Collected data were analyzed by FlowJo software (Tree Star).

ChIP Assay

ChIP assay was previously described (Yamagishi et al., 2009). Briefly, cells were crosslinked with 1% of formaldehyde, sonicated, and subjected to chromatin-conjugated IP using specific antibodies. Precipitated DNA was purified and analyzed by real-time PCR with specific primers (see Supplemental Experimental Procedures).

Computational Prediction

To identify miR-31 target genes, we integrated the output results of multiple prediction programs; TargetScan, PicTar, miRanda, and PITA. RNAhybrid was for secondary structure of miRNA-3′ UTR hybrid. TSSG program was for TATA box and TSS predictions. DNA methylation site was predicted by CpG island Searcher.

Statistical Analyses

Data were analyzed as follows: (1) Welch's t test for Gene Expression Microarray (p value cutoff at 10^{-6}) and miRNA Microarray (p value cutoff at 10^{-5}); (2) Pearson's correlation for two-dimensional hierarchical clustering analysis and individual assessment of microarray data sets; (3) two-tailed pared Student's t test with $p < 0.05$ considered statistically significant for in vitro cell lines and primary cells experiments, including luciferase assay, RT-PCR, ChIP assay, cell growth assay, and migration assay. Data are presented as mean ± SD.

ACCESSION NUMBERS

Coordinates have been deposited in Gene Expression Omnibus database with accession numbers, GSE31629 (miRNA microarray), GSE33615 (gene expression microarray), and GSE33602 (copy number analyses).

SUPPLEMENTAL INFORMATION

Supplemental Information includes three tables, five figures, and Supplemental Experimental Procedures and can be found with this article online at doi:10.1016/j.ccr.2011.12.015.

ACKNOWLEDGMENTS

We thank Dr. M. Iwanaga, Mr. M. Nakashima, and Ms. T. Akashi for support and maintenance of JSPFAD. We thank Drs. H. Miyoshi and A. Miyawaki for providing the Venus-encoding lentivirus vectors. We also thank Dr. R. Horie for experimental advices, and Drs. T. Kanno and T. Ishida for providing the MDA-MB-453. Grant support: Grants-in-Aid for Scientific Research from Ministry of Education, Culture, Sports, Science, and Technology of Japan to T.W. (No. 23390250) and by Grants-in-Aid from the Ministry of Health, Labour and Welfare to T.W. (H21-G-002 and H22-AIDS-I-002).

Received: November 3, 2010
Revised: August 12, 2011
Accepted: December 19, 2011
Published: January 17, 2012

REFERENCES

Annunziata, C.M., Davis, R.E., Demchenko, Y., Bellamy, W., Gabrea, A., Zhan, F., Lenz, G., Hanamura, I., Wright, G., Xiao, W., et al. (2007). Frequent engagement of the classical and alternative NF-kappaB pathways by diverse genetic abnormalities in multiple myeloma. Cancer Cell *12*, 115–130.

Bartel, D.P. (2009). MicroRNAs: target recognition and regulatory functions. Cell *136*, 215–233.

Bellon, M., Lepelletier, Y., Hermine, O., and Nicot, C. (2009). Deregulation of microRNA involved in hematopoiesis and the immune response in HTLV-I adult T-cell leukemia. Blood *113*, 4914–4917.

Caretti, G., Di Padova, M., Micales, B., Lyons, G.E., and Sartorelli, V. (2004). The Polycomb Ezh2 methyltransferase regulates muscle gene expression and skeletal muscle differentiation. Genes Dev. *18*, 2627–2638.

Chen, Y., Takita, J., Choi, Y.L., Kato, M., Ohira, M., Sanada, M., Wang, L., Soda, M., Kikuchi, A., Igarashi, T., et al. (2008). Oncogenic mutations of ALK kinase in neuroblastoma. Nature *455*, 971–974.

Davis, B.N., Hilyard, A.C., Lagna, G., and Hata, A. (2008). SMAD proteins control DROSHA-mediated microRNA maturation. Nature *454*, 56–61.

Fiskus, W., Wang, Y., Sreekumar, A., Buckley, K.M., Shi, H., Jillella, A., Ustun, C., Rao, R., Fernandez, P., Chen, J., et al. (2009). Combined epigenetic therapy with the histone methyltransferase EZH2 inhibitor 3-deazaneplanocin A and the histone deacetylase inhibitor panobinostat against human AML cells. Blood *114*, 2733–2743.

Hayden, M.S., and Ghosh, S. (2008). Shared principles in NF-kappaB signaling. Cell *132*, 344–362.

Hironaka, N., Mochida, K., Mori, N., Maeda, M., Yamamoto, N., and Yamaoka, S. (2004). Tax-independent constitutive IkappaB kinase activation in adult T-cell leukemia cells. Neoplasia *6*, 266–278.

Horie, R., Watanabe, M., Ishida, T., Koiwa, T., Aizawa, S., Itoh, K., Higashihara, M., Kadin, M.E., and Watanabe, T. (2004). The NPM-ALK oncoprotein

abrogates CD30 signaling and constitutive NF-kappaB activation in anaplastic large cell lymphoma. Cancer Cell *5*, 353–364.

Iwanaga, M., Watanabe, T., Utsunomiya, A., Okayama, A., Uchimaru, K., Koh, K.R., Ogata, M., Kikuchi, H., Sagara, Y., Uozumi, K., et al; Joint Study on Predisposing Factors of ATL Development investigators. (2010). Human T-cell leukemia virus type I (HTLV-1) proviral load and disease progression in asymptomatic HTLV-1 carriers: a nationwide prospective study in Japan. Blood *116*, 1211–1219.

Kleer, C.G., Cao, Q., Varambally, S., Shen, R., Ota, I., Tomlins, S.A., Ghosh, D., Sewalt, R.G., Otte, A.P., Hayes, D.F., et al. (2003). EZH2 is a marker of aggressive breast cancer and promotes neoplastic transformation of breast epithelial cells. Proc. Natl. Acad. Sci. USA *100*, 11606–11611.

Liao, G., Zhang, M., Harhaj, E.W., and Sun, S.C. (2004). Regulation of the NF-kappaB-inducing kinase by tumor necrosis factor receptor-associated factor 3-induced degradation. J. Biol. Chem. *279*, 26243–26250.

Malinin, N.L., Boldin, M.P., Kovalenko, A.V., and Wallach, D. (1997). MAP3K-related kinase involved in NF-kappaB induction by TNF, CD95 and IL-1. Nature *385*, 540–544.

Min, J., Zaslavsky, A., Fedele, G., McLaughlin, S.K., Reczek, E.E., De Raedt, T., Guney, I., Strochlic, D.E., Macconaill, L.E., Beroukhim, R., et al. (2010). An oncogene-tumor suppressor cascade drives metastatic prostate cancer by coordinately activating Ras and nuclear factor-kappaB. Nat. Med. *16*, 286–294.

Prasad, S., Ravindran, J., and Aggarwal, B.B. (2010). NF-kappaB and cancer: how intimate is this relationship. Mol. Cell. Biochem. *336*, 25–37.

Ramakrishnan, P., Wang, W., and Wallach, D. (2004). Receptor-specific signaling for both the alternative and the canonical NF-kappaB activation pathways by NF-kappaB-inducing kinase. Immunity *21*, 477–489.

Saitoh, Y., Yamamoto, N., Dewan, M.Z., Sugimoto, H., Martinez Bruyn, V.J., Iwasaki, Y., Matsubara, K., Qi, X., Saitoh, T., Imoto, I., et al. (2008). Overexpressed NF-kappaB-inducing kinase contributes to the tumorigenesis of adult T-cell leukemia and Hodgkin Reed-Sternberg cells. Blood *111*, 5118–5129.

Sander, S., Bullinger, L., Klapproth, K., Fiedler, K., Kestler, H.A., Barth, T.F., Möller, P., Stilgenbauer, S., Pollack, J.R., and Wirth, T. (2008). MYC stimulates EZH2 expression by repression of its negative regulator miR-26a. Blood *112*, 4202–4212.

Schaefer, A., Jung, M., Mollenkopf, H.J., Wagner, I., Stephan, C., Jentzmik, F., Miller, K., Lein, M., Kristiansen, G., and Jung, K. (2010). Diagnostic and prognostic implications of microRNA profiling in prostate carcinoma. Int. J. Cancer *126*, 1166–1176.

Simon, J.A., and Kingston, R.E. (2009). Mechanisms of polycomb gene silencing: knowns and unknowns. Nat. Rev. Mol. Cell Biol. *10*, 697–708.

Sparmann, A., and van Lohuizen, M. (2006). Polycomb silencers control cell fate, development and cancer. Nat. Rev. Cancer *6*, 846–856.

Su, I.H., Basavaraj, A., Krutchinsky, A.N., Hobert, O., Ullrich, A., Chait, B.T., and Tarakhovsky, A. (2003). Ezh2 controls B cell development through histone H3 methylation and Igh rearrangement. Nat. Immunol. *4*, 124–131.

Su, I.H., Dobenecker, M.W., Dickinson, E., Oser, M., Basavaraj, A., Marqueron, R., Viale, A., Reinberg, D., Wülfing, C., and Tarakhovsky, A. (2005). Polycomb group protein ezh2 controls actin polymerization and cell signaling. Cell *121*, 425–436.

Suh, J., and Rabson, A.B. (2004). NF-kappaB activation in human prostate cancer: important mediator or epiphenomenon? J. Cell. Biochem. *91*, 100–117.

Thu, Y.M., and Richmond, A. (2010). NF-κB inducing kinase: a key regulator in the immune system and in cancer. Cytokine Growth Factor Rev. *21*, 213–226.

Trabucchi, M., Briata, P., Garcia-Mayoral, M., Haase, A.D., Filipowicz, W., Ramos, A., Gherzi, R., and Rosenfeld, M.G. (2009). The RNA-binding protein KSRP promotes the biogenesis of a subset of microRNAs. Nature *459*, 1010–1014.

Valastyan, S., Reinhardt, F., Benaich, N., Calogrias, D., Szász, A.M., Wang, Z.C., Brock, J.E., Richardson, A.L., and Weinberg, R.A. (2009). A pleiotropically acting microRNA, miR-31, inhibits breast cancer metastasis. Cell *137*, 1032–1046.

Varambally, S., Dhanasekaran, S.M., Zhou, M., Barrette, T.R., Kumar-Sinha, C., Sanda, M.G., Ghosh, D., Pienta, K.J., Sewalt, R.G., Otte, A.P., et al. (2002). The polycomb group protein EZH2 is involved in progression of prostate cancer. Nature *419*, 624–629.

Varambally, S., Cao, Q., Mani, R.S., Shankar, S., Wang, X., Ateeq, B., Laxman, B., Cao, X., Jing, X., Ramnarayanan, K., et al. (2008). Genomic loss of microRNA-101 leads to overexpression of histone methyltransferase EZH2 in cancer. Science *322*, 1695–1699.

Ventura, A., and Jacks, T. (2009). MicroRNAs and cancer: short RNAs go a long way. Cell *136*, 586–591.

Watanabe, M., Ohsugi, T., Shoda, M., Ishida, T., Aizawa, S., Maruyama-Nagai, M., Utsunomiya, A., Koga, S., Yamada, Y., Kamihira, S., et al. (2005). Dual targeting of transformed and untransformed HTLV-1-infected T cells by DHMEQ, a potent and selective inhibitor of NF-kappaB, as a strategy for chemoprevention and therapy of adult T-cell leukemia. Blood *106*, 2462–2471.

Yamagishi, M., Ishida, T., Miyake, A., Cooper, D.A., Kelleher, A.D., Suzuki, K., and Watanabe, T. (2009). Retroviral delivery of promoter-targeted shRNA induces long-term silencing of HIV-1 transcription. Microbes Infect. *11*, 500–508.

Yamaguchi, K., and Watanabe, T. (2002). Human T lymphotropic virus type-I and adult T-cell leukemia in Japan. Int. J. Hematol. *76* (*Suppl 2*), 240–245.

Yeung, M.L., Yasunaga, J., Bennasser, Y., Dusetti, N., Harris, D., Ahmad, N., Matsuoka, M., and Jeang, K.T. (2008). Roles for microRNAs, miR-93 and miR-130b, and tumor protein 53-induced nuclear protein 1 tumor suppressor in cell growth dysregulation by human T-cell lymphotrophic virus 1. Cancer Res. *68*, 8976–8985.

Zarnegar, B.J., Wang, Y., Mahoney, D.J., Dempsey, P.W., Cheung, H.H., He, J., Shiba, T., Yang, X., Yeh, W.C., Mak, T.W., et al. (2008a). Noncanonical NF-kappaB activation requires coordinated assembly of a regulatory complex of the adaptors cIAP1, cIAP2, TRAF2 and TRAF3 and the kinase NIK. Nat. Immunol. *9*, 1371–1378.

Zarnegar, B.J., Yamazaki, S., He, J.Q., and Cheng, G. (2008b). Control of canonical NF-kappaB activation through the NIK-IKK complex pathway. Proc. Natl. Acad. Sci. USA *105*, 3503–3508.

Int J Hematol (2011) 94:430–434
DOI 10.1007/s12185-011-0934-4

Current status of HTLV-1 infection

Toshiki Watanabe

Received: 10 August 2011 / Revised: 31 August 2011 / Accepted: 2 September 2011 / Published online: 4 October 2011

Abstract It is 30 years since human T-cell leukemia virus type 1 (HTLV-1) was identified as the first human retrovirus. To assess the implications of the virus for human health it is very important to know the past and present prevalence. Most of the estimates of HTLV-1 prevalence are based on serological screening of blood donors, pregnant women and other selected population groups. The widely cited estimate that the number of HTLV-1 carriers in Japan is 1.2 million was calculated from data that are now more than 25 years old. Here I summarize previous reports of prevalence studies in the world and Japan. Then, a recent analysis of seroprevalence of healthy blood donors in Japan will be described in comparison with that of 1988. A decrease in the number of HTLV-1 carriers in Japan was demonstrated, however, it is still more than one million. The number has increased in the metropolitan areas, probably reflecting the migration of Japanese population. I conclude that there is a paucity of general population data in countries where HTLV-1 is endemic, and re-evaluation of HTLV-1 infection is required to understand the virus burden on the human health.

Keywords Seroprevalence of HTLV-1 · Vertical and horizontal transmission · Prevention of transmission

1 Introduction

Discovery of adult T-cell leukemia (ATL) by Takatsuki's group [1] was followed by the discovery of the first human retrovirus human T-cell leukemia virus (HTLV) and adult T-cell leukemia virus (ATLV) by research groups of the United State and Japan, respectively [2, 3]. In 1980, Poiesz et al. [2] identified HTLV in a T-cell line from a patient with cutaneous T-cell lymphoma. Independently of this, Hinuma and Miyoshi found specific antibodies against ATL cells in the patients' sera [3] and type C retrovirus particles produced by a T-cell line established from peripheral blood of ATL patient in 1981 [4]. In 1982, Yoshida et al. [5] identified ATLV as a human retrovirus. Soon, HTLV and ATLV were shown to be identical at the sequence level and were named HTLV type 1 (HTLV-1) [6, 7].

After the discovery of HTLV-1, related viruses have been isolated and HTLV is now composed of 4 related HTLVs, HTLV-1 to HTLV-4 [8]. However, only HTLV-1 has been convincingly linked to human diseases at present. HTLV-1 has six reported subtypes (subtypes A–F). Diverse studies have been performed on HTLV-1 subtyping but present a minor role in the epidemiological status of the virus. The great majority of infections are caused by the cosmopolitan subtype A, and there is no report of subtype influence on the pathogenic potential of HTLV-1 [9].

2 HTLV-1 infection in the world

Approximately 20 million people worldwide are estimated to be infected with HTLV-1 [10]. Among them, more than 90% remain asymptomatic carriers during their lives. Since 1986, HTLV-1 screening has been developed and was slowly implemented worldwide [11]. In 1993, HTLV-1 screening of blood donors was already performed in all developed countries and in many developing countries where HTLV-1 is endemic.

T. Watanabe (✉)
Department of Medical Genome Sciences,
Graduate School of Frontier Sciences, The University of Tokyo,
4-6-1 Shirokanedai, Minato-ku, Tokyo 108-8639, Japan
e-mail: tnabe@ims.u-tokyo.ac.jp

About the geographic distribution of the virus, a lot of studies have been done in these 30 years. Results indicate that Japan, Africa, the Caribbean islands, and Central and South America are the areas of highest prevalence in the world (reviewed in [12], [13]). However, the data from international prevalence studies should be interpreted and compared with caution as to the population selection criteria, because any difference in the diagnostic strategies can interfere with the final result. Data of the serological screening of healthy blood donors mainly provide basis for the estimation of the global prevalence of HTLV-1, which tends to underestimate the prevalence in the population. The geographic distribution of HTLV-1 infection is shown in Fig. 1 [13].

In addition to Japan, high rates of HTLV-1 infection have been reported for some Caribbean islands in studies of blood donors or segments of the general population. In Jamaica, the prevalence is around 5%. In Africa, the seroprevalence increases from the north to the south, varying from 0.6% in Morocco to greater than 5% in several sub-Saharan African countries, for example, Benin, Cameroon, and Guinea-Bissau, however, more studies are clearly required about these regions in detail. In Europe and North America, the prevalence is low and limited to groups that emigrated from endemic areas. For blood donors, very low rates were found in France (0.0039%) and the United States (0.025%). In South America, the virus was found in all countries, but more studies of the general population are needed to ascertain the real prevalence of HTLV-1. Medium prevalence was found in blood donors from Chile (0.73%) and Argentina (0.07%). In Australia, a prevalence of 14% was reported in a cluster among Aborigines in the Northern Territory, even though the prevalence in blood donors is low. The prevalence of HTLV-1 was highest in the two studies of Japanese islands (36.4%) and lowest in studies from Mongolia, Malaysia and India. In Haiti the prevalence was 3.8%; in Africa between 6.6 and 8.5% in Gabon, and 1.05% in Guinea. Only three studies were from West Africa and none were from the South; the only study from India was from the north of the country. It has to be

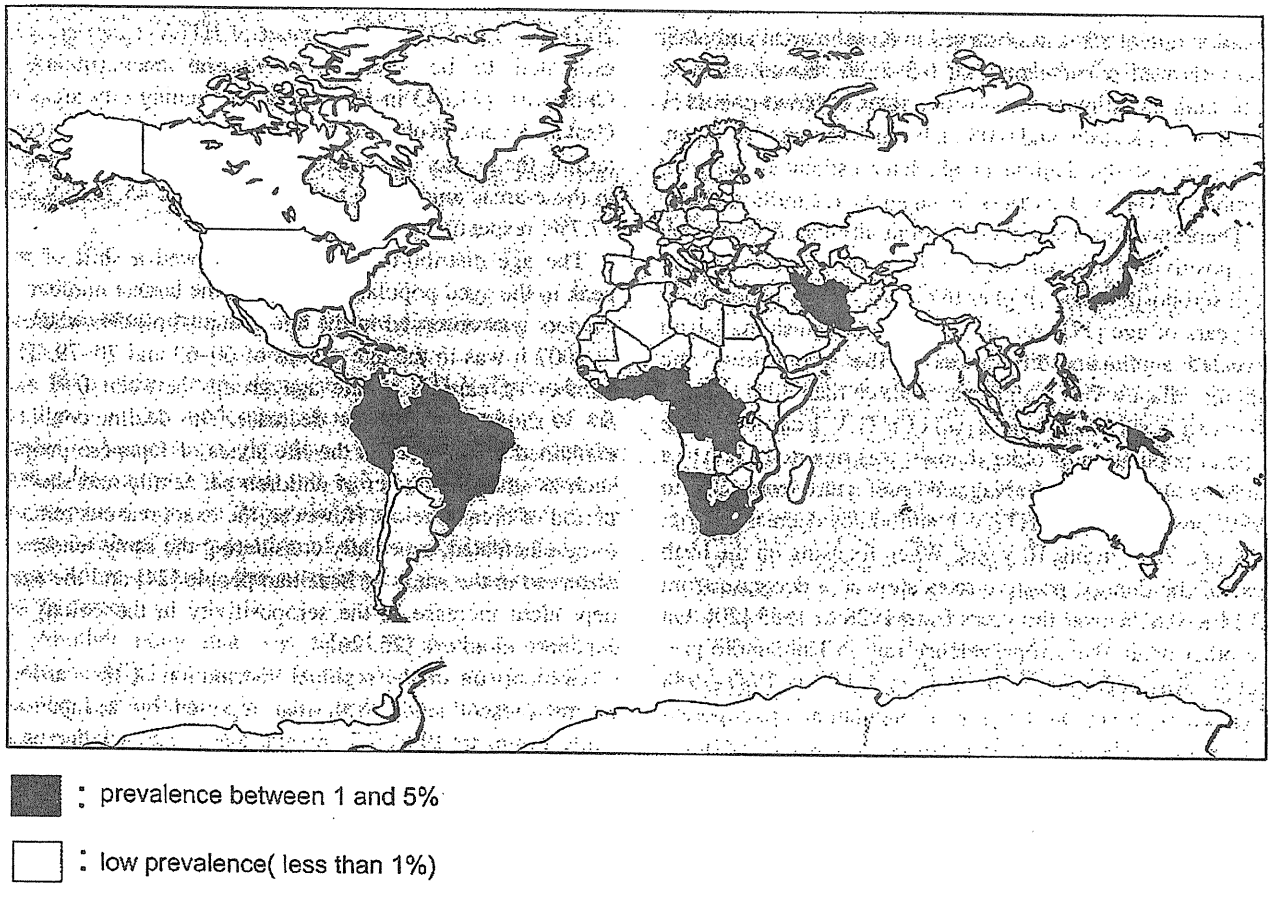

Fig. 1 Countries with endemic HTLV-I, defined as prevalence between 1 and 5% in some populations, are shown in *red*. Countries with reports of low prevalence (less than 1% in some groups), due mainly to immigration from endemic areas, are shown in *yellow*. It should be noted that HTLV-I endemic areas do not correspond exactly to the country boundaries shown in the map, for example, Brazil, Japan and Iran, where HTLV-I is limited to residents of certain areas of each country (modified from the reference [13])

concluded that there is a paucity of general population data from countries in which HTLV-1 is endemic, and that new studies are required to reevaluate the global burden of infection (reviewed in ref. [12] and [13]).

3 HTLV-1 Infection in Japan

3.1 Past studies of HTLV-1 carriers

Many efforts have been made to know the number of HTLV-1 carriers since the discovery of the virus in Japan. An example of early nationwide studies is the report of seropositive rates in the 15 blood centers of Japanese Red Cross [14]. It was reported that among 15 blood centers, 7 showed a higher positive rates between 6 and 30%, tested by indirect immunofluorescence assays (IFA). The other report is based on the data of all blood centers in Japan, which was the only study of all areas of Japan before the resent survey by Satake et al. [15]. They studied by IFA about 15,000 samples composed of 200 samples of blood donors aged from 40 to 64 from each center. The highest positive rate of 8% was observed in Kyushu area, and other areas showed positive rates of 0.3–1.2%. Based on these data, authors estimate seropositive rates of blood donors as about 3% in Kyushu and 0.08–0.3% in other areas of Japan. Using this study, Tajima et al., later estimated the total number of HTLV-1 carriers in Japan as 1.2 million [16].

There have been reports of community-based studies on seropositivities in Japan. One of the studies reported a very high seropositive rate (higher than 40%) in the people over 40 years of age [17]. An old study of the Tsushima Island revealed significant differences in the seropositive rate among villages with a high rate of more than 30% [18]. In Okinawa, a very high rate (21%) of HTLV-1 carriers in the general population of older than 40 was reported [19]. In a study of blood donors in Nagasaki prefecture from 1990 to 1999, positive rate of HTLV-1 antibodies decreased from 3.39 to 2.78% during 10 years. When focusing on the birth year of the donors, positive rates showed a decrease from 13.14 to 0.81% over the years from 1928 to 1983 [20]. On the other hand, the seroprevalence rate in Kumamoto prefecture was reported to be 3.6 or 4.7% in 1987–1988 [21, 22]. A survey on the general population was reported in Hokkaido. The average seropositive rate was 0.8% (male 0.6% and female 0.9%), with some regions showing higher seroprevalence rates as much as 5.2% [23].

Taken together, studies in 1980s and 1990s were mostly community-based ones using sera of blood donors. The oldest nationwide survey of the seroprevalence of HTLV-1 in blood donors and estimation of the number of HTLV-1 carriers [15, 16] had been referred to as the only published information until recently.

3.2 Recent studies of HTLV-1 infection in Japan

Based on the numbers of seropositive blood donors, Satake et al. have estimated the number of HTLV-1 carriers in Japan [15]. They analyzed data of blood donors who donated for the first time in 2006 and 2007, because Japanese Red Cross Blood center has notified the donors with the results of screening tests since 2000. This notification would have caused a bias in the population of total blood donors reducing the number of HTLV-1 carriers. In Satake's study, the total of number of tested was 1,196,321 (M: 704,074; F: 492,247), among them, HTLV-1 antibody was confirmed to be positive in 37,787 (M: 2,115; F: 1,672). Thus, the positive ratio was 0.32% for both male and female. Since the ages of blood donors were limited between 16 and 64, they estimated the seropositive rates of the peoples of younger than 15 or older than 65 by an assumption that the positive rate will increase exponentially in the young population, and for the aged people, by adding the average increase in the percentage in each age group in 20 years comparing with the data in 1988. Consequently, the estimated number of HTLV-1 carriers in 2007 was 1,078,722. The number of HTLV-1 carriers was estimated to be 492,582 in Kyushu area (including Okinawa), 171,843 in Kinki area (containing city areas of Osaka, Kyoto, Kobe) and 190,609 in Kanto area (containing the greater Tokyo area). The percentages of carriers in these areas among the total carriers were 45.7, 15.9 and 17.7%, respectively.

The age distribution of carriers showed a shift of the peak to the aged population. In 1988, the largest number of carriers was observed in the age group of 50–59, whereas in 2007 it was in the age groups of 60–69 and 70–79. The number of carriers in the age groups between 0–9 and 50–59 showed a significant decrease. This decline could be explained by changes in the life styles of Japanese people such as smaller number of children per family and shorter period of breast feeing. However, the exact reasons remain to be elucidated, especially considering the same tendency observed in the study of Brazilian people [24] and the age-dependent increase in the seropositivity in the colony of Japanese monkeys [25, 26].

Comparison of the regional distribution of the carriers in the present study with that reported by a Japanese study group in 1990 [27] revealed a significant decrease of the HTLV-1 carriers in Kyushu area (50.9 to 45.7%) and an increase in Kanto area (10.8 to 17.7%). The observed changes were considered to be mainly due to the migration of Japanese people from the Kyushu/Okinawa area to the metropolitan areas (Fig. 2). This interpretation is supported by the observation of Uchimaru et al. [28], who studied HTLV-1 carriers in Tokyo area and revealed that many of HTLV-1 carriers in Tokyo are either born in

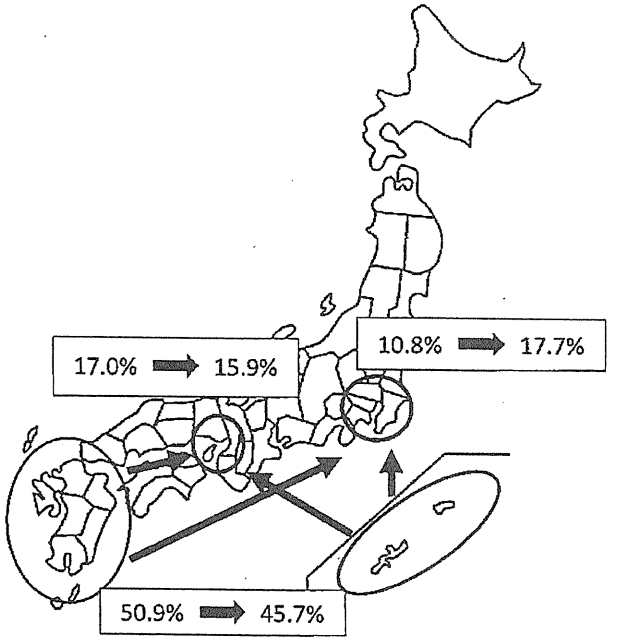

Fig. 2 Distribution of HTLV-1 carriers in Japan. Migration to the metropolitan areas is apparent. The number of HTLV-1 carriers in the endemic areas is still the largest, however, those in the great Tokyo area is significantly increasing

the endemic areas or the descendants of migrants from those areas.

4 Remaining problems and future directions

We have attributed the decrease in the HTLV-1 prevalence in Japan to the modernization and westernization of life styles of Japanese people. However, when we consider the same tendency in Brazil and age-dependent increase of seropositive rates in Japanese monkeys, we have to be cautious about interpretation of the observed data and may have to re-evaluate the meaning of the age-dependent carrier rates.

Another point that was raised by Satake's study is unexpectedly high increase in the positive rates in 20 years in the age-cohort [15]. This indicates the presence of horizontal transmission of the virus, probably through sexual contacts. This mode of infection should have contributed, at least to some extent, to the age-dependent increase in the positive rates. Thus, epidemiological studies on the horizontal transmission are definitely required; however, no such studies are now under way in Japan.

Taken together, we have to realize that we do not have enough data about the prevalence of HTLV-1 even in Japan, where serological data of blood donors are the only information to estimate the prevalence. Serological screening of the pregnant women that started in 2011 will provide valuable information about young females in Japan. Since the number of carriers who develop ATL is estimated about 1,200 per year in Japan, we have to expect more than 20,000 ATL patients from the present carriers in the future. In addition to the screening for the blood donors, prevention of mother-to-child infection by stopping breast feeding will greatly reduce the vertical transmission, nonetheless, there still remain other modalities of HTLV-1 infection, that are sexual transmission and possible trans-uterine infection. Neutralizing antibodies are often observed in carriers of HTLV-1 [29–32]. Furthermore, previous reports suggest that a primed immune response can be protective or prevent infection postviral exposure and challenge. It was shown that maternally acquired antibody protect infants from HTLV-1 infection in the early months of life [33]. A vaccine candidate based on an envelope expressing vaccinia virus provides protection to experimentally challenged primates [34, 35], and an attenuated viral strain provides long-term protection against the closely related bovine leukemia virus [36]. Taking all these into consideration, a costeffective vaccine may be a viable objective for prophylactic intervention in HTLV-1-endemic areas.

References

1. Uchiyama T, Yodoi J, Sagawa K, Takatsuki K, Uchino H. Adult T-cell leukemia: clinical and hematologic features of 16 cases. Blood. 1977;50:481–92.
2. Poiesz BJ, Ruscetti FW, Gazdar AF, Bunn PA, Minna JD, Gallo RC. Detection and isolation of type C retrovirus particles from fresh and cultured lymphocytes of a patient with cutaneous T-cell lymphoma. Proc Natl Acad Sci USA. 1980;77:7415–9.
3. Hinuma Y, Nagata K, Hanaoka M, Nakai M, Matsumoto T, Kinoshita KI, et al. Adult T-cell leukemia: antigen in an ATL cell line and detection of antibodies to the antigen in human sera. Proc Natl Acad Sci USA. 1981;78:6476–80.
4. Miyoshi I, Kubonishi I, Yoshimoto S, Akagi T, Ohtsuki Y, Shiraishi Y, et al. Type C virus particles in a cord T-cell line derived by co-cultivating normal human cord leukocytes and human leukaemic T cells. Nature. 1981;294:770–1.
5. Yoshida M, Miyoshi I, Hinuma Y. Isolation and characterization of retrovirus from cell lines of human adult T-cell leukemia and its implication in the disease. Proc Natl Acad Sci USA. 1982;79:2031–5.
6. Watanabe T, Seiki M, Yoshida M. Retrovirus terminology. Science. 1983;222:1178.
7. Gallo RC. History of the discoveries of the first human retroviruses: HTLV-1 and HTLV-2. Oncogene. 2005;24:5626–930.
8. Mahieux R, Gessain A. The human HTLV-3 and HTLV-4 retroviruses: new members of the HTLV family. Pathol Biol (Paris). 2009;57:161–6.
9. Ono A, Miura T, Araki S, Yamaguchi K, Takatsuki K, Mori S, et al. Subtype analysis of HTLV-1 in patients with HTLV-1 uveitis. Jpn J Cancer Res. 1994;85:767–70.

10. de Thé G, Kazanji M. An HTLV-I/II vaccine: from animal models to clinical trials? J Acquir Immune Defic Syndr Hum Retrovirol. 1996;13(Suppl 1):S191–8.
11. Inaba S, Sato H, Okochi K, Fukada K, Takakura F, Tokunaga K, et al. Prevention of transmission of human T lymphotropic virus type 1 (HTLV-1) through transfusion, by donor screening with antibody to the virus. One-year experience. Transfusion. 1989;29: 7–11.
12. Goncalves DU, Proietti FA, Ribas JGR, Araujo MG, Pinheiro SR, Guedes AC, et al. Epidemiology, treatment, and prevention of human T-cell leukemia virus type 1-associated diseases. Clin Microbiol Rev. 2010;23:577–89.
13. Proietti FA, Anna Bárbara, Carneiro-Proietti F, Bernadette C, Catalan-Soares, Murphy EL, et al. Global epidemiology of HTLV-I infection and associated diseases. Oncogene. 2005;24: 6058–68.
14. Hinuma Y, Komoda H, Chosa T, Kondo T, Kohakura M, Takenaka T, et al. Antibodies to adult T-cell leukemia-virus-associated antigen (ATLA) in sera from patients with ATL and controls in Japan: a nation-wide sero-epidemiologic study. Int J Cancer. 1982;29:631–5.
15. Satake M, Yamaguchi K. Annual report of the group study for survey of HTLV-1 infection and HTLV-1 related diseases in Japan. 2009 (in Japanese) (Manuscript submitted).
16. Tajima K. The 4th nation-wide study of adult T-cell leukemia/lymphoma (ATL) in Japan: estimates of risk of ATL and its geographical and clinical features. The T- and B-cell Malignancy Study Group. Int J Cancer. 1990;45:237–43.
17. Kohakura M, Nakada K, Yonahara M, Komoda H, Imai J, Hinuma Y. Seroepidemiology of the human retrovirus (HTLV/ATLV) in Okinawa where adult T-cell leukemia is highly endemic. Jpn J Cancer Res. 1986;77:21–3.
18. Tajima K, Kamura S, Ito S, Ito M, Nagatomo M, Kinoshita K, Ikeda S. Epidemiological features of HTLV-I carriers and incidence of ATL in an ATL-endemic island: a report of the community-based co-operative study in Tsushima, Japan. Int J Cancer. 1987;40:741–6.
19. Kohakura M, Nakada K, Yonahara M, Komoda H, Imai J, Hinuma Y. Seroepidemiology of the human retrovirus (HTLV/ATLV) in Okinawa where adult T-cell leukemia is highly endemic. Jpn J Cancer Res. 1986;77:21–3.
20. Chiyoda S, Kinoshita K, Egawa S, Inoue J, Watanabe K, Ifuku M. Decline in the positive rate of human T-lymphotropic virus type-1 (HTLV-1) antibodies among blood donors in Nagasaki. Intern Med. 2001;40:14–7.
21. Lee SY, Mastushita K, Machida J, Tajiri M, Yamaguchi K, Takatsuki K. Human T-cell leukemia virus type I infection in hemodialysis patients. Cancer. 1987;60:1474–8.
22. Iida S, Fujiyama S, Yoshida K, Morishita T, Shibata J, Sato T, et al. The seroprevalence of anti-HTLV-1 antibodies in patients with various liver diseases. Hepatogastroenterol. 1988;35:242–4.
23. Kwon KW, Yano M, Sekiguchi S, Iwanaga M, Fujiwara S, Oikawa O, et al. Prevalence of human T-cell leukemia virus type 1 (HTLV-I) in general inhabitants in non-adult T-cell leukemia (ATL)-endemic Hokkaido, Japan. In Vivo. 1994;8:1011–4.
24. Barcellos NT, Fuchs SC, Mondini LG, Murphy EL. Human T lymphotropic virus type I/II infection: prevalence and risk factors in individuals testing for HIV in counseling centers from Southern Brazil. Sex Transm Dis. 2006;33:302–6.
25. Ishida T, Yamamoto K, Kaneko R, Tokita E, Hinuma Y. Seroepidemiological study of antibodies to adult T-cell leukemia virus-associated antigen (ATLA) in free-ranging Japanese monkeys (Macaca fuscata). Microbiol Immunol. 1983;27:297–301.
26. Hayami M, Komuro A, Nozawa K, Shotake T, Ishikawa K, Yamamoto K, et al. Prevalence of antibody to adult T-cell leukemia virus-associated antigens (ATLA) in Japanese monkeys and other non-human primates. Int J Cancer. 1984;33:179–83.
27. Tajima K, Itoh S, Itoh T, Kinoshita K, Shimotohno K. Epidemiology of ATL and HTLV-1. In: the annual report of the group study "Inhibition of mother-to-child infection and ATL" (1990). 1991 (in Japanese).
28. Uchimaru K, Nakamura Y, Tojo A, Watanabe T, Yamaguchi K. Factors predisposing to HTLV-1 infection in residents of the greater Tokyo area. Int J Hematol. 2008;88:565–70.
29. Astier-Gin T, Portail JP, Londos-Gagliardi D, Moynet D, Blanchard S, Dalibart R, et al. Neutralizing activity and antibody reactivity toward immunogenic regions of the human T cell leukemia virus type I surface glycoprotein in sera of infected patients with different clinical states. J Infect Dis. 1997;175:716–9.
30. Londos-Gagliardi D, Armengaud MH, Freund F, Dalibart R, Moze E, Huet S, et al. Antibodies directed against a variable and neutralizable region of the HTLV-I envelope surface glycoprotein. Leukemia. 1997;11(Suppl. 3):38–41.
31. Hadlock KG, Rowe J, Perkins S, Bradshaw P, Song GY, Cheng C, et al. Neutralizing human monoclonal antibodies to conformational epitopes of human T-cell lymphotropic virus type 1 and 2 gp46. J Virol. 1997;71:5828–40.
32. Hadlock KG, Rowe J, Foung SK. The humoral immune response to human T-cell lymphotropic virus type 1 envelope glycoprotein gp46 is directed primarily against conformational epitopes. J Virol. 1999;73:1205–12.
33. Takahashi K, Takezaki T, Oki T, Kawakami K, Yahiski S, Fujiyoshi T, et al. Inhibitory effect of maternal antibody on mother-to-child transmission of human T-lymphotropic virus type I. Int J Cancer. 1991;49:673–7.
34. Kazanji M, Heraud JM, Merien F, Pique C, de The G, Gessain A, Jacobson S, et al. Chimeric peptide vaccine composed of B- and T-cell epitopes of human T-cell leukemia virus type 1 induces humoral and cellular immune responses and reduces the proviral load in immunized squirrel monkeys (*Saimiri sciureus*). J Gen Virol. 2006;87:1331–7.
35. Kazanji M, Tartaglia J, Franchini G, de Thoisy B, Talarmin A, Contamin H, Gessain A, de The G, et al. Immunogenicity and protective efficacy of recombinant human T-cell leukemia/lymphoma virus type 1 NYVAC and naked DNA vaccine candidates in squirrel monkeys (*Saimiri sciureus*). J Virol. 2001;75:5939–48.
36. Kerkhofs P, Gatot JS, Knapen K, Mammerickx M, Burny A, Portetelle D, Willems L, Kettmann R. Long-term protection against bovine leukaemia virus replication in cattle and sheep. J Gen Virol. 2000;81:957–63.

Leukemia (2012) 1 - 9

www.nature.com/leu

ORIGINAL ARTICLE

Clinical significance of CADM1/TSLC1/IgSF4 expression in adult T-cell leukemia/lymphoma

S Nakahata[1], Y Saito[1], K Marutsuka[2], T Hidaka[3], K Maeda[3,4], K Hatakeyama[5], T Shiraga[1,6], A Goto[1], N Takamatsu[1], Y Asada[5], A Utsunomiya[7], A Okayama[8], Y Kubuki[3], K Shimoda[3], Y Ukai[9], G Kurosawa[9] and K Morishita[1]

Cell adhesion molecule 1 (CADM1/TSLC1) was recently identified as a novel cell surface marker for adult T-cell leukemia/lymphoma (ATLL). In this study, we developed various antibodies as diagnostic tools to identify CADM1-positive ATLL leukemia cells. In flow cytometric analysis, the percentages of $CD4^+CADM1^+$ double-positive cells correlated well with both the percentages of $CD4^+CD25^+$ cells and with abnormal lymphocytes in the peripheral blood of patients with various types of ATLL. Moreover, the degree of $CD4^+CADM1^+$ cells over 1% significantly correlated with the copy number of the human T-lymphotropic virus type 1 (HTLV-1) provirus in the peripheral blood of HTLV-1 carriers and ATLL patients. We also identified a soluble form of CADM1 in the peripheral blood of ATLL patients, and the expression levels of this form were correlated with the levels of soluble interleukin 2 receptor alpha. Moreover, lymphomas derived from ATLL were strongly and specifically stained with a CADM1 antibody. Thus, detection of $CD4^+CADM1^+$ cells in the peripheral blood, measurement of serum levels of soluble CADM1 and immunohistochemical detection of CADM1 in lymphomas would be a useful set of markers for disease progression in ATLL and may aid in both the early diagnosis and measurement of treatment efficacy for ATLL.

Leukemia advance online publication, 6 January 2012; doi:10.1038/leu.2011.379

Keywords: CADM1/IgSF4/TSLC1; ATLL

INTRODUCTION

Adult T-cell leukemia/lymphoma (ATLL) results from infection with human T-lymphotropic virus type 1 (HTLV-1).[1,2] Following HTLV-1 infection, 2.1 to 6.6% of HTLV-1 carriers will develop ATLL, and most of the ATLL patients will die within a year.[3] An estimated 10–20 million people worldwide are infected with HTLV-1, and HTLV-1 is endemic in southwestern Japan, the island of Kyushu, Africa, the Caribbean Islands and South America.[4] ATLL cells are mainly derived from activated helper T cells with the $CD3^+$, $CD4^+$, $CD8^-$ and $CD25^+$ (also known as interleukin 2 receptor alpha (IL-2Rα)) cell surface markers.[2] A fraction of ATLL cases have been shown to also express forkhead box P3 (*FOXP3*), which is a master gene for regulatory T cells (T-reg), suggesting that some cases of ATLL may originate from HTLV-1-infected T-reg cells.[5,6] For diagnosis, identification of mono- or oligoclonal provirus integration events by Southern blot analysis is one of the definitive markers for ATLL. In addition to viral integration, ATLL cells with multi-lobulated nuclei (called 'flower cells') have been frequently seen in leukemia cells in the peripheral blood of ATLL patients. Hypercalcemia and high levels of either serum lactate dehydrogenase (LDH) or soluble IL-2Rα (sIL-2Rα) have been found to be unfavorable markers for ATLL; however, these markers are not specific for the diagnosis of ATLL.[7,8]

The developmental steps of ATLL after HTLV-1 infection have remained obscure for 30–40 years. HTLV-1 Tax is thought to be an important viral protein that functions in the maintenance of HTLV-1-infected lymphocytes;[9,10] however, expression of Tax protein was not detected in over 70% of ATLL cases because of genomic deletion and/or DNA methylation.[11–14] Recently, HTLV-1 basic leucine zipper (HBZ) was found to be constitutively expressed in ATLL cells and was shown to interact with JUN and CREB2 to regulate Tax expression.[15,16] HBZ also promotes $CD4^+$ T-cell proliferation in transgenic mice;[16] therefore, HBZ has important roles and functions not only in maintaining the virus life cycle but also in the maintenance of the HTLV-1-infected cells that contribute to disease pathogenesis. Although HBZ is expressed in the majority of ATLL cells, only 5% of HTLV-1 carriers develop ATLL, suggesting that additional factors besides viral infection are required for the development of ATLL.

To identify additional pathogenic factors or novel surface markers for ATLL, we collected gene expression profiles for acute-type ATLL. Using a comprehensive DNA microarray gene expression analysis, we recently demonstrated that cell adhesion molecule 1 (CADM1/TSLC1/IgSF4) is a novel cell surface maker for ATLL.[17] CADM1 was initially isolated as a tumor suppressor for lung cancers by genomic analysis. CADM1 expression is reduced in a variety of cancers by promoter methylation and is associated with poor prognosis and enhanced metastatic potential.[18] By contrast, we identified that high expression of CADM1 has an important role in enhanced cell–cell adhesion to the vascular endothelium, tumor growth and the organ infiltration of ATLL cells.[19]

In this study, we developed various antibodies for CADM1 to be used as diagnostic tools for identifying ATLL leukemia cells.

[1]Division of Tumor and Cellular Biochemistry, Department of Medical Sciences, Faculty of Medicine, University of Miyazaki, Miyazaki, Japan; [2]Pathology Division, University of Miyazaki Hospital, Miyazaki, Japan; [3]Department of Gastroenterology and Hematology, Faculty of Medicine, Miyazaki University, Miyazaki, Japan; [4]Department of Internal Medicine, Miyakonojo National Hospital, Miyazaki, Japan; [5]Department of Pathology, Faculty of Medicine, University of Miyazaki, Miyazaki, Japan; [6]Department of Foods and Human Nutrition, Faculty of Human Life Sciences, Notre Dame Seishin University, Okayama, Japan; [7]Department of Hematology, Imamura Bun-in Hospital, Kagoshima, Japan; [8]Department of Rheumatology, Infectious Diseases and Laboratory Medicine, University of Miyazaki, Miyazaki, Japan and [9]Division of Antibody Project, Institute for Comprehensive Medical Science, Fujita Health University, Aichi, Japan. Correspondence: Professor K Morishita, Division of Tumor and Cellular Biochemistry, Department of Medical Science, Faculty of Medicine, University of Miyazaki, 5200 Kihara, Kiyotake, Miyazaki 889-1692, Japan.
E-mail: kmorishi@med.miyazaki-u.ac.jp
Received 14 April 2011; revised 24 November 2011; accepted 29 November 2011